AGU ADVANCING EARTH AND SPACE SCIENCES

Water Resources Research

RESEARCH ARTICLE
10.1029/2023WR035443

Quantifying the Impact of Human Activities on Hydrological Drought and Drought Propagation in China Using the PCR-GLOBWB v2.0 Model

Xiaoli Yang[1,2], Fan Wu[1,2], Shanshui Yuan[1,3,4], Liliang Ren[1,2], Justin Sheffield[5], Xiuqin Fang[1,2], Shanhu Jiang[1,2], and Yi Liu[1,2]

[1]The National Key Laboratory of Water Disaster Prevention, Hohai University, Nanjing, China, [2]College of Hydrology and Water Resources, Hohai University, Nanjing, China, [3]Yangtze Institute for Conservation and Development, Hohai University, Nanjing, China, [4]Key Laboratory of Hydrologic-Cycle and Hydrodynamic-System of Ministry of Water Resources, Hohai University, Nanjing, China, [5]Geography and Environment, University of Southampton, Southampton, UK

Key Points:

- We used the PCR-GLOBWB v2.0 model to study the impact of human activities on the process of drought propagation
- Human activities play a varying role in the propagation process of drought in different river basins
- Human activities has led to a decrease in drought propagation rates and shortened/prolonging the drought lag time in northern/southern China

Supporting Information:

Supporting Information may be found in the online version of this article.

Correspondence to:

S. Yuan,
yuanshanshui@hhu.edu.cn

Citation:

Yang, X., Wu, F., Yuan, S., Ren, L., Sheffield, J., Fang, X., et al. (2024). Quantifying the impact of human activities on hydrological drought and drought propagation in China using the PCR-GLOBWB v2.0 model. *Water Resources Research*, *60*, e2023WR035443. https://doi.org/10.1029/2023WR035443

Received 29 MAY 2023
Accepted 22 DEC 2023

Abstract The economic and human losses caused by drought are increasing, driven by climate change, human activities, and increased exposure of livelihood activities in water-dependent sectors. Mitigation of these impacts for socio-ecological securit is necessary to gain a better understanding of how human activities contribute to the propagation of drought as water management further develops. The previous studies investigated the impact of human activities on a macro level, but they overlooked the specific effects caused by human water management measures. In addition, most studies focus on the propagation time (PT, the number of months from meteorological drought propagation to hydrological drought), while other drought propagation characteristics, such as duration, magnitude, and recovery time, are not yet sufficiently understood. To tackle these issues, the PCR-GLOBWB v2.0 hydrological model simulated hydrological processes in China under natural and human-influenced scenarios. The study assessed how human activities impact hydrological drought and its propagation. Result shows that human activities have exacerbated hydrological drought in northern China, while it is mitigated in the south. The propagation rate (PR, proportion of meteorological drought propagation to hydrological drought) ranges from 45% to 75%, and the PT is 6–23 months. The PR does not differ substantially between the north and south, while the PT is longer in the north. The PR decreases by 1%–60% due to human activities, and the PT decreases (1–13 months) in the north and increases (1–10 months) in the south. Human activities display significant variations in how they influence the propagation process of drought across different basins. The primary factors driving the spatial pattern of drought disparities are regional variations in irrigation methods and the storage capacity of reservoirs.

Plain Language Summary Under the combined impact of climate change and human activities, economic and human losses caused by drought in China have been increasing year by year. To mitigate the impact of disasters, we conducted research using PCR-GLOBWB v2.0 model to investigate how human activities have altered hydrological drought in China. And the role of human activities in the propagation process of drought was explored. The results indicate that human activities have intensified hydrological drought in northern China, while providing some alleviation in the southern regions. Human activities disrupt the natural processes of drought propagation, resulting in a decrease in propagation rates. Furthermore, human activities have shortened the propagation lag time of drought in the north, while increasing it in the south. Additionally, smaller basins are more sensitive to human activities compared to larger basins. Our study reveals the impact of human activities on hydrological drought and drought propagation, providing valuable insights for the development of more effective drought adaptation strategies.

1. Introduction

Drought is a naturally occurring hydrometerological event caused by chronic water shortage (He et al., 2020; Hunt et al., 2014; Long et al., 2023; Xu et al., 2015). Drought can have devastating impacts on agriculture, ecology, and society, and is recognized as one of the world's most severe and widespread types of disasters (He et al., 2019; Kao & Govindaraju, 2010; Logan et al., 2010; Markonis et al., 2021; Peng et al., 2020; Wilhite et al., 2014; Xu et al., 2021; Zhang et al., 2015). The global socio-economic cost of drought is approximately US$250 to $300 billion per year and is increasing annually (FAO, 2018). In recent decades, China has suffered from prolonged and

severe droughts, posing a serious threat to food and water security while causing huge socio-economic losses (Wu et al., 2011; Yu et al., 2014). For example, severe droughts occurred in southwestern China from the summer of 2009 to the spring of 2010, leading to crop failures on over 4 million hectares and causing water shortages for 16 million people. The severe drought of 2011 triggered a dramatic drop or even complete drying up of lake levels in the affected areas and severe water shortages for crops and cities, with total losses of $2.3 billion (Jin et al., 2013). Therefore, the study of drought issues warrants continued attention (Huang et al., 2015).

Droughts can be generally classified into meteorological, agricultural, hydrological and socioeconomic droughts according to different hydrological cycle deficits (American Meteorological Society, 1997; He & Sheffield, 2020; Van Loon & Laaha, 2015; World Meteorological Organization, 2006). Meteorological droughts are usually associated with negative precipitation anomalies (Leng & Tang, 2014); agricultural droughts are generally triggered by declining soil moisture; reduced local surface runoff or groundwater recharge will lead to hydrological drought (Wada et al., 2013; Wu et al., 2018); socioeconomic drought occurs when drought events cause socioeconomic impacts (Zhao et al., 2019). Previous research has found associations between different type of droughts, mostly focusing on meteorological and hydrological droughts, given that hydrological droughts often have the widest impacts across multiple sectors (Apurv et al., 2017; Guo et al., 2020; Han et al., 2019; He et al., 2017; Herrera-Estrada et al., 2017; Huang et al., 2017; S. Liu et al., 2019; Van Loon et al., 2012; Wu et al., 2017). In general, meteorological drought serves as the source of all droughts, impacting hydrological drought through connections in the water cycle, a process known as drought propagation. Better understanding of the propagation process can enable timely forecasting of hydrological drought, which, in turn, aids in establishing early warning systems for water resources management and mitigating the impacts of drought.

There is a lag-time from meteorological drought propagation to hydrological drought. Barker et al. (2016) calculated drought propagation time (PT) in 121 natural catchments in the UK using the Standardized Precipitation Index (SPI) and the Standardized Streamflow Index (SSI). The results indicate that the PT is longer in the southern and eastern parts of the UK, while the opposite is observed in the western and northern regions. Huang et al. (2017) found that PT in the Weihe River basin has distinct seasonal characteristics. El Niño Southern Oscillation (ENSO) and Arctic Oscillation (AO) are closely related to PT. Most of the existing studies focus on the PT of meteorological to hydrological drought, while there are other complex relationships in the drought propagation process (Van Loon & Laaha, 2015). PT only represents the lag-time characteristics of drought propagation, ignoring other important drought characteristics (e.g., duration, magnitude, and recovery time), which can be an important basis for measuring drought damage. Consideration of the structure and characteristics of drought propagation should also include the drought propagation rate (PR, proportion of meteorological drought propagation to hydrological drought), duration (drought onset to end), magnitude (level of drought), and recovery time (drought peak to end). In this study, the propagation characteristics of various drought features are considered, which can better reveal the propagation process and help deepen understanding all-round.

In previous studies, drought propagation has been usually considered as a natural phenomenon. However, with increasing human activities in recent years, drought events cannot be considered as purely natural events (AghaKouchak et al., 2015; Lorenzo-Lacruz et al., 2013). Thus, the drivers of drought occurrence, development, and recovery cannot be considered as a natural process, but have shifted to a combination of natural and human factors (i.e., climate change and human activities) (Jiang et al., 2019; Van Loon et al., 2016). A few studies have considered the effects of human activities on drought, and there are roughly four ways to estimate the human impact: (a) the "upstream-downstream" comparison method (Rangecroft et al., 2019); (b) the "runoff mutation point" method; (c) the "paired sub-basins" method (Van Loon et al., 2019); (d) the "stem and tributary comparison" method (Li et al., 2021; Wang et al., 2020). However, the above methods are only applicable to small watersheds or their applicability is constrained by various conditions. In addition, human activities affect drought propagation in various ways, and these methods cannot quantify the efffect of human activities, such as water extraction, irrigation, and reservoir scheduling.

Compared with the above methods, modeling approaches can be considered more useful and widely applicable. They can be used to explicitly separate out natural and human factors, albeit with uncertainties in how well the model represents the observed world. Hydrological models can comprehensively reveal the spatiotemporal changes of drought, which is why they are increasingly favored (Omer et al., 2020; Zhu et al., 2019). Many hydrological models consider human activities to some extent, but they still focus on simulating rainfall-runoff and make considerable generalizations about human activities, such as the widely used SWAT and VIC models

(Tallaksen et al., 2009; Van Loon et al., 2016). However, these models do not fully consider human activities such as water abstraction, irrigation, and reservoir regulation, which greatly affects their simulation accuracy. Therefore, in the process of constructing hydrological models, fully considering the feedback relationship between human activities and hydrological processes is essential. It represents a more effective research approach for quantitatively analyzing the impact of human activities on hydrological drought.

The PCR-GLOBWB hydrological model developed by Utrecht University has been used to quantify the impact of human activities on the terrestrial water cycle (De Graaf et al., 2014; He et al., 2017; Sutanudjaja et al., 2018; Van Beek et al., 2011; Wada et al., 2014). The PCR-GLOBWB v2.0 model (Sutanudjaja et al., 2018) is an improved version of the PCR-GLOBWB1.0, which is a grid-based large-scale hydrological model with fine spatial resolution (5 arcmin). The model is able to independently assess water demand and water availability, representing the vast majority of human activities that affect the water cycle, for example, groundwater abstraction, irrigation (paddy and non-paddy irrigation), human water abstraction (subdivided into domestic, livestock, and industrial water needs), desalination, reservoir dispatch, etc. The model runs on a daily step. It can simulate the terrestrial water cycle from catchment to continental or even global scale. The model has become a valuable tool for understanding the impacts of climate change and human activities on water resources (Cheng et al., 2021; De Graaf et al., 2019; Jiao et al., 2020; Sutanudjaja et al., 2018; Yang et al., 2020).

Most previous studies have qualitatively described the effects of human activities on hydrological drought and drought propagation (Sattar et al., 2019; Wang et al., 2020), and such effects have not been quantified and fully understood. Therefore, this study explores the impact of human activities on drought in China using the PCR-GLOBWB v2.0 model. We conduct two scenarios (natural scenario and scenario considering human influences, hereafter referred to as NatSim and AnthrSim) and simulated the water cycle processes. The aim is to determine the contribution of human activities to hydrological drought and drought propagation, and how natural and human factors lead to differences in drought.

2. Data and Study Area

According to the principles of China's water resources classification by the Resource and Environment Data Center of the Chinese Academy of Sciences (http://www.resdc.cn), the Chinese mainland is divided into nine major river basins. These regions are: Songliao River Basin (SRB), Haihe River Basin (HARB), Huaihe River Basin (HURB), Yellow River Basin (YERB), Yangtze River Basin (YZRB), Zhujiang Basin (ZRB), Dongnan basin (DRB), Xinan basin (XRB) and Neilu Basin (NRB), corresponding to numbers 1–9 in Figure 1.

Daily meteorological observations from 1961 to 2020 (including temperature and precipitation) were obtained from 756 meteorological stations, provided by the National Climate Center (NCC) of the China Meteorological Administration (CMA). We applied the inverse distance weight interpolation method to interpolate the station data to a 5 arcmin (~10 km) grid and use this to force the PCR-GLOBWB v2.0 model. The model operates based on a water balance, allowing for the calculation of reference potential evapotranspiration according to the Hamon method with only daily average temperature (Sutanudjaja et al., 2018). The potential evapotranspiration for specific crops is calculated within the model using crop factors from different land cover types as outlined in the Food and Agriculture Organization (FAO) guidelines. Subsequently, the actual evapotranspiration for specific crops is determined based on their potential evapotranspiration. In addition to calculating evapotranspiration, another role of temperature is to distinguish between precipitation in the form of rain and snow. The other input data for the PCR-GLOBWB v2.0 model will be introduced in Section 3.1.1.

We obtained daily discharge observations from 30 hydrological stations (2007–2015) from the Annual Hydrological Report of the People's Republic of China, which were used to evaluate the PCR-GLOBWB v2.0 model's performance. The geographical locations of the hydrological and the meteorological stations are shown in Figure 1. Furthermore, annual data for domestic, industrial, and irrigation water use for each province in China (2007–2015) are collected from the Ministry of Water Resources of the People's Republic of China (http://www.mwr.gov.cn/). These data were utilized to validate the accuracy of the model in representing human water withdrawals.

3. Methodology

In order to quantify the impacts of human activities on hydrological drought and drought propagation, we propose the following analytical framework (Figure 2). It is comprised of five major parts. (a) We used the PCR-GLOBWB

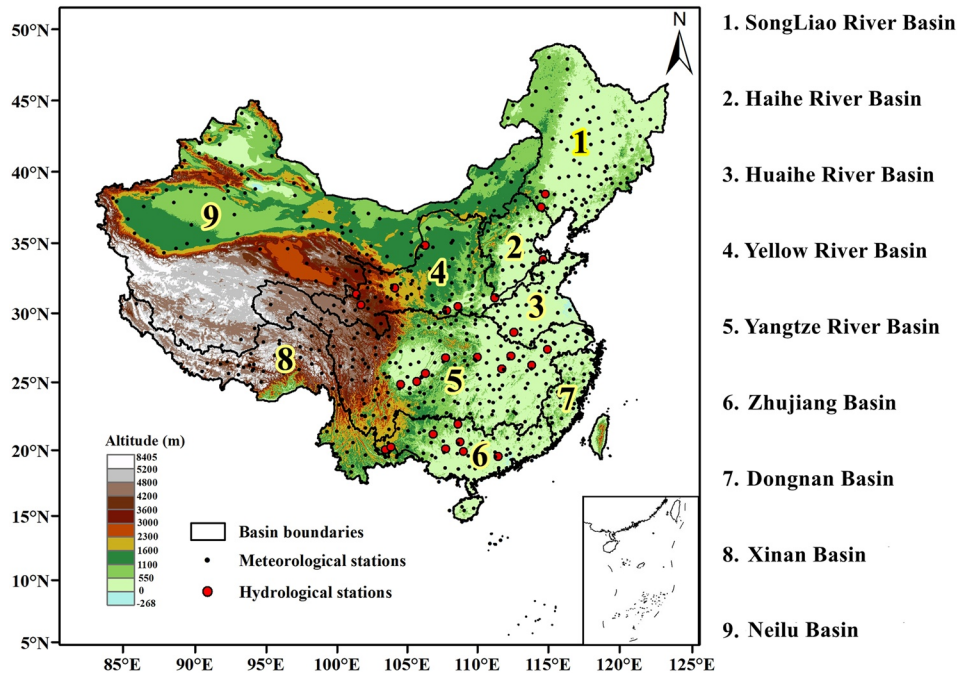

Figure 1. Locations of nine major basins, 30 hydrological stations and 756 meteorological stations in China. The altitude data in the figure is sourced from the Institute of Geographic Sciences and Natural Resources Research, Chinese Academy of Sciences (https://www.resdc.cn/Datalist1.aspx?FieldTyepID=9,13).

v2.0 model to simulate the terrestrial water cycle under NatSim and AnthrSim. (b) The difference in hydrological drought between the two scenarios was quantified based on the Standardized Runoff Index (SRI) and run theory. (c) The PT and PR from meteorological to hydrological drought were then obtained by matching drought events, and correlation analysis. (d) Linear and nonlinear drought propagation models were constructed to reveal how hydrological drought responds to the meteorological drought. (e) Cross-wavelet analysis was used to explore the potential reasons for differences in hydrological drought from both natural factors (including precipitation, evapotranspiration, and soil moisture) and human factors (irrigation water use, groundwater extraction, and human domestic and industrial water consumption).

3.1. Discharge Simulation Under NatSim and AnthrSim

3.1.1. PCR- GLOBWB v2.0 Model

The PCR-GLOBWB v2.0 model (Sutanudjaja et al., 2018) is an improved version of the PCR-GLOBWB 1.0 model for assessing water scarcity at global scale. It is a state-of-the-art gridded global hydrological and water resources model. Compared to the PCR-GLOBWB 1.0 model, it has higher spatial resolution (5 arcmin), which means that it can more depict the fine spatial variability of surface parameters such as water routing, soil and vegetation and more accurately simulate terrestrial hydrological cycle processes (Bierkens et al., 2015; Pan & Wood, 2010). The model's inputs and parameter database primarily include meteorological drivers, upper and lower soil store parameters, land cover types, topographical parameters, root fractions per soil layer, parameters related to phenology, groundwater parameters, and so on. In this study, all inputs and parameters except for meteorological drivers are sourced from Wada et al. (2013, 2014, 2016) and Sutanudjaja et al. (2018).

In addition, the PCR-GLOBWB v2.0 model includes modules for water demand (domestic, industrial, livestock) and irrigation. These modules fully consider the impacts of human water withdrawals, encompassing demand, abstraction, net consumption, and return processes. Domestic water demand is calculated by multiplying the population (FAO AQUASTAT, http://www.fao.org/nr/water/aquastat/main/index.stm) in a single grid by the domestic water quotas for the region (FAO, 2016). Industrial water demand is not affected by seasons and remains constant throughout the year. The method for calculating the livestock water demand is to multiply the livestock density in a single grid (FAOSTAT, http://faostat.fao.org/) by the livestock water quota. The population, livestock density, and water quotas of each region vary year by year, which reflects that human water usage changes over

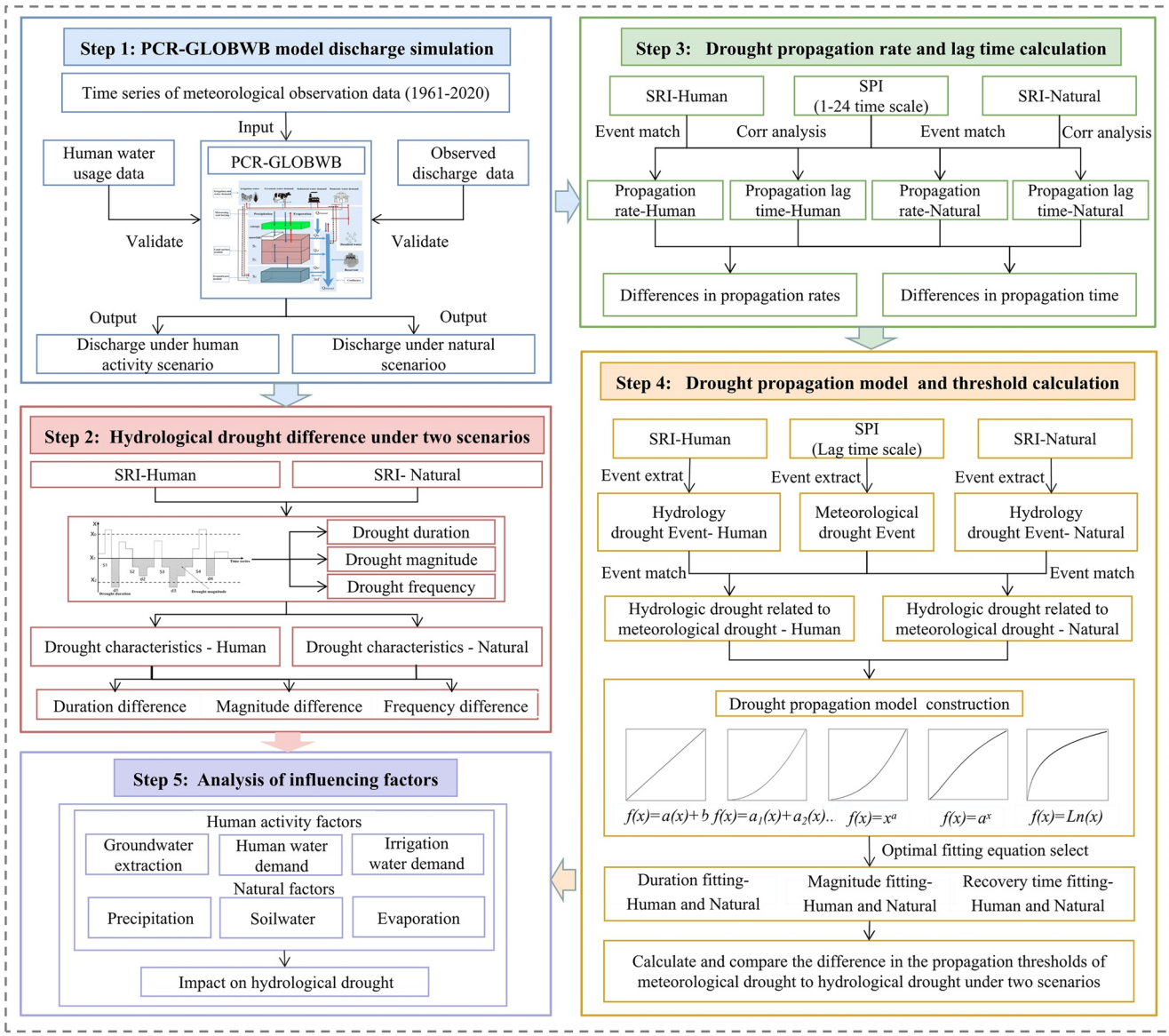

Figure 2. A framework based on the PCR-GLOBWB v2.0 model for isolating the effects of human activities on drought and drought propagation. Note: The conceptual diagram of the model is cited from Sutanudjaja et al. (2018).

time. The gridded data set required to drive the model for domestic water use is sourced from the Food and Agriculture Organization AQUASTAT database (http://www.fao.org/nr/water/aquastat/main/index.stm). Industrial water use data are obtained from Shiklomanov (1997), WRI (1998), and Vörösmarty et al. (2005). Livestock water use data are sourced from the Food and Agriculture Organization (2007) and Steinfeld et al. (2006). The irrigation guidelines follow FAO rules (FAO, 2003), distinguishing between paddy and non-paddy irrigation and formulating corresponding crop regimes. The reservoir module considers the needs of human water use, drought resistance, irrigation, etc. The operating rules of the reservoir use a forward-looking scheme (Wada et al., 2014), assessing local and downstream water demand conditions to develop a dynamic water supply scheme (Van Beek et al., 2011).

The PCR-GLOBWB v2.0 model has a flexible modular structure, and the link connecting each module is the mutual conversion process of water (Yang et al., 2020). The modular components can be modified and replaced according to specific goals, allowing activation of the reservoir regulation, irrigation and different water use modules to simulate the hydrological process under the influence of human activities (Cheng et al., 2021; Wu et al., 2024). These refined settings make the PCR-GLOBWB v2.0 model an ideal choice for simulating the

impact of human activities on terrestrial hydrological processes. More details about the model can be found in Wada et al. (2013, 2014, 2016) and Sutanudjaja et al. (2018).

3.1.2. Scenario Settings

The main objective of this study was to evaluate the effect of human activities on hydrological drought and drought propagation, so two experimental scenarios were set up. The first scenario was to run the PCR-GLOBWB v2.0 model without any human activities to simulate the terrestrial water cycle process in the natural state. The second scenario includes human activity components of the model (human water use, irrigation water, reservoir scheduling), simulating human influenced hydrological processes under the same meteorological forcing conditions of the NatSim. These two scenarios are simulated independently, and they start simulating subsequent years only after the model has achieved stability through the spin-up process. This ensures that there is no interference from previous periods or between scenarios.

3.1.3. Model Validation

In order to evaluate the PCR-GLOBWB v2.0 model's performance, we calculated the Nash-Sutcliffe coefficient (NSE; Nash & Sutcliffe, 1970) of the discharge between the model simulation (AnthrSim) and the observations from 30 hydrological stations in China. Water level decline and reduced flow are considered as the primary factors leading to hydrological drought, with low flow phenomenon particularly exerting significant influence on hydrological drought. To comprehensively assess model performance, the Kling-Gupta Efficiency (KGE, Gupta et al., 2009; Kling et al., 2012) coefficient is used to evaluate the simulation performance of low-flow events (Q90, which represents the 90% exceedance of the long-term average daily flow). In addition, the accuracy of human activity data is primarily measured through the quantification of Relative Bias (BIAS) and root mean square errors (RMSE) between model simulations and statistical data.

3.2. Drought Measurement and Characteristic Identification

3.2.1. Standardized Precipitation Index

We use the Standardized Precipitation Index (SPI) to characterize meteorological drought (Mckee et al., 1993). The SPI takes into account the precipitation within a specific time frame (Xu et al., 2019). The principle is to normalize precipitation using a specific probability distribution function to measure the degree of drought (Faiz et al., 2018). SPI is temporally flexible and can be applied to precipitation deficits at different time scales (1, 3, 6, 12, 24 months) to characterize cumulative drought conditions. The SPI is calculated as follows:

$$f(x) = \frac{1}{\beta\Gamma(\alpha)} x^{\alpha-1} e^{\frac{-x}{\beta}} \tag{1}$$

Where, x is the precipitation in a certain time period; Γ is the gamma distribution function; α and β are shape and scale parameters of Γ function.

$$F(X) = \int_0^x f(x)dx \tag{2}$$

Where, $F(x)$ is the cumulative probability distribution of precipitation, which is normalized to obtain the SPI.

$$\mathrm{SPI} = -\left(k - \frac{c_0 + c_1 k + c_2 k^2}{1 + d_1 k + d_2 k^2 + d_3 k^3}\right), k = \sqrt{\ln\left[\frac{1}{F(x)^2}\right]}, 0 < F(x) \le 0.5 \tag{3}$$

$$\mathrm{SPI} = k - \frac{c_0 + c_1 k + c_2 k^2}{1 + d_1 k + d_2 k^2 + d_3 k^3}, k = \sqrt{\ln\left[\frac{1}{1 - F(x)^2}\right]}, 0.5 < F(x) \le 1 \tag{4}$$

Where, $c_0 = 2.515517$, $c_1 = 0.802853$, $d_1 = 1.432788$, $d_2 = 0.189269$, $d_3 = 0.001308$.

3.2.2. Standardized Runoff Index

The Standardized Runoff Index (SRI) was proposed by Shukla and Wood (2008). It follows the SPI calculation principle and only requires replacing the input variable precipitation with discharge. As with SPI, it is spatially comparable and temporally flexible.

3.2.3. Run Theory

Run theory is a threshold-based method that defines drought events as values less than the threshold, and extracts events from the drought index series. The schematic diagram of run theory is shown in Figure S1 in Supporting Information S1. In this study, the thresholds of SPI and SRI were set at −0.5 to identify the meteorological and hydrological drought characteristics, including the drought duration (e.g., M_D1 represents the duration of meteorological drought event 1), the drought event frequency (the number of drought events that occurred during the study period) and the drought magnitude (e.g., H_M1 represents the magnitude of hydrological drought event 1). Furthermore, in order to fully characterize drought propagation, the drought event recovery time (RP, defined as the time difference between the drought peak point and the drought recovery point) was extracted.

3.3. Correlation Analysis

3.3.1. Drought Propagation Lag Time and Propagation Rate

Typically, hydrological droughts are triggered by meteorological droughts, which results in a lag time between them. The Pearson Correlation Coefficient (CC) is one of the most commonly used methods for calculating PT in previous studies (Barker et al., 2016; Hellwig et al., 2020; Huang et al., 2019; Xu et al., 2019). The method involves cross-correlating the hydrological drought index at a specific time scale (e.g., 1-month time scale SRI) with the meteorological drought index at different time scales (e.g., 1, 2, 3…n-month time scales SPI). The time scale corresponding to the highest cross-correlation (CC) was then taken as the propagation time (PT). The study area covers the entire China, and there are large differences in natural conditions among different basins, so the time scale of SPI is extended to 1–24 months. We cross-correlated the SPI-n with SRI-1 in the NatSim and AnthrSim, respectively, to obtain the spatial distribution of PT in the two scenarios.

Drought propagation rate is represented by the ratio of hydrological drought propagated by meteorological drought. A higher propagation rate indicates a greater sensitivity of hydrological drought in the region to meteorological drought, implying a closer connection between the two. A lower propagation percentage suggests a lesser extent of meteorological drought propagating to hydrological drought. The mathematical expression for drought propagation rate is as follows:

$$\mathrm{PR} = \frac{n}{m} \tag{5}$$

Where, PR represents the drought propagation rate, where n signifies the count of hydrological drought events in response to meteorological drought events, and m represents the total number of meteorological drought events during the study period. Note: Due to the existence of the drought propagation time relationship, when calculating the propagation rate statistically, SPI-n sequences corresponding to the time scale of the propagation time in that area should be selected.

3.3.2. Drought Characteristic Propagation Model

The process of the drought characteristics propagation model is described as follows. First, we matched the SPI-n (n is the time scale corresponding to PT) with SRI to identify the one-to-one corresponding meteorological and hydrological drought events, and extracted their drought characteristics via run theory. Second, drawing on the method proposed by Wu et al. (2017), two types (linear and nonlinear) of models are constructed. The linear model includes univariate linear regression, and the nonlinear model includes multiple regression, exponential function, power function and logarithmic function (Figure 2). Finally, we fit and analyzed drought characteristics, and selected the model with the highest coefficient of determination (R^2) as the best fit.

3.3.3. Wavelet Analysis

Wavelet analysis (Hudgins et al., 1993) is an effective tool for exploring the correlation between two time series. It's a novel technique that combines cross-spectral analysis and wavelet transform, allowing the revelation of the interaction and correlation between two signals at different time scales. Therefore, we utilize Cross Wavelet Transform (XWT) to uncover the connection between influencing factors and hydrological drought.

The cross wavelet power spectrum between X and Y is defined as:

$$W_j^{XY}(s) = W_j^X(s) W_j^{Y*}(s) \tag{6}$$

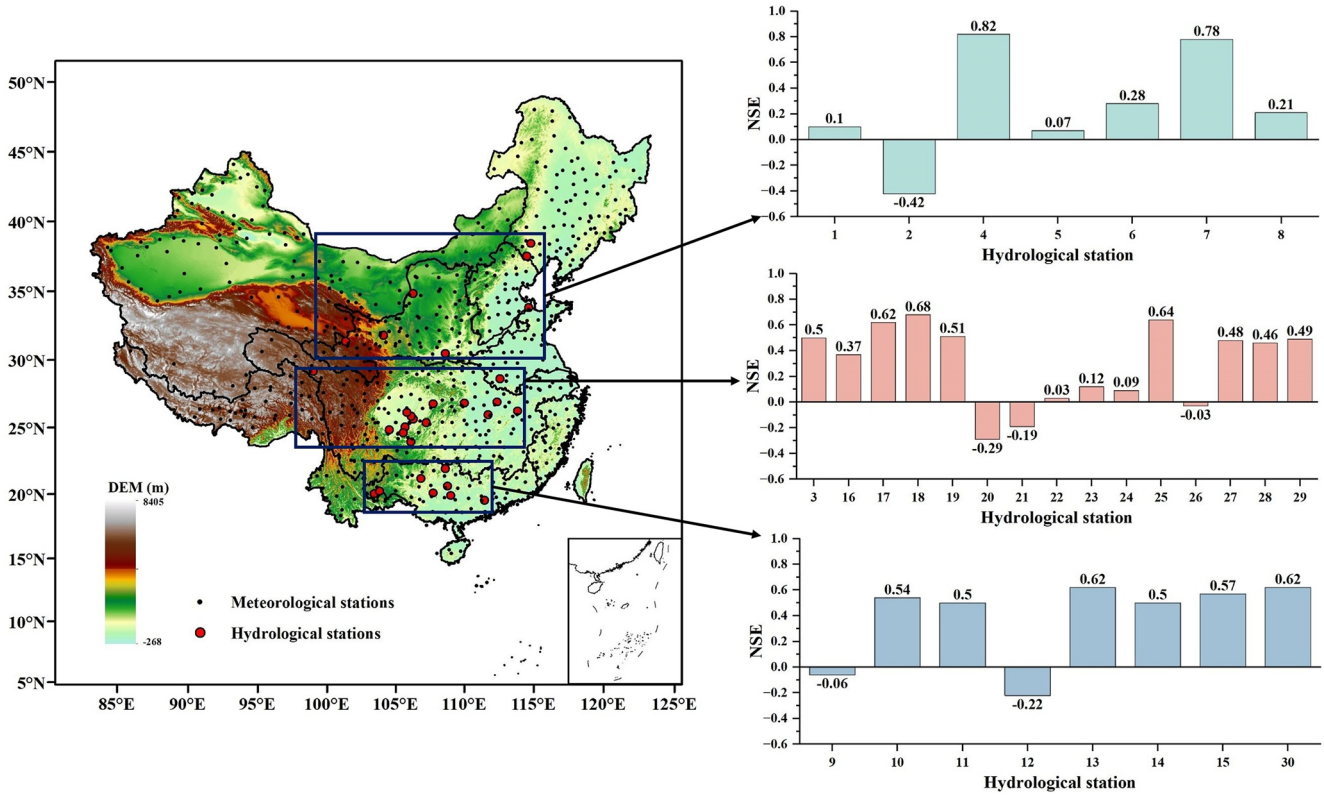

Figure 3. Nash-Sutcliffe coefficients (NSE) for simulated monthly flows and observed monthly flow rates (m^3/s) at 30 stations for the AnthrSim and their spatial locations for the period 2007–2015. The number of the hydrological station corresponds to the information in Table S1 in Supporting Information S1.

Where $W_j^{XY}(s)$ is the cross wavelet transform result of X and Y; $W_j^X(s)$ is the continuous wavelet transform result of X; $W_j^{Y*}(s)$ is the complex conjugate of $W_j^X(s)$; and s *is* the frequency scale. It should be noted that in this article, X represents the time series of the modeled human activity or natural factors, while Y represents the time series of hydrological drought.

The wavelet coherence is defined as:

$$R_j^2(s) = \frac{\left|S\left(s^{-1}W_j^{XY}(s)\right)\right|^2}{S\left(s^{-1}\left|W_j^X(s)\right|^2\right)S\left(s^{-1}\left|W_j^Y(s)\right|^2\right)} \quad (7)$$

Where, $R_j^2(s)$ is the wavelet coherence result of X and Y; S is the smoothing operator.

4. Results

The NSE coefficients suggest that the model's performance in China is generally satisfactory (Table S1 in Supporting Information S1). The model performs better in the south than north, which might be due to lack of accurate snowmelt simulation and higher uncertainties in precipitation in dryland (Figure 3). Overall, the PCR-GLOBWB v2.0 model can the simulate large-scale terrestrial hydrological cycle and reproduce the monthly discharge well across China.

Figure S2 in Supporting Information S1 displays the KGE values and Correlation Coefficients (CC) for simulations and observations of Q90 at 30 hydrological stations. Among them, KGE values at more than 20 sites exceed 0.6, and the simulation performance is better under AnthrSim compared to NatSim. CC for 27 stations exceed 0.8, demonstrating a strong fitting trend between simulated and observed water flows. Overall, the PCR-GLOBWB v2.0 model effectively captures the variations and patterns of low flow at most stations.

Figure S3 in Supporting Information S1 compares model simulations against observational data for human water usage. Due to data limitations, the assessment was conducted only at the annual scale. Despite some differences

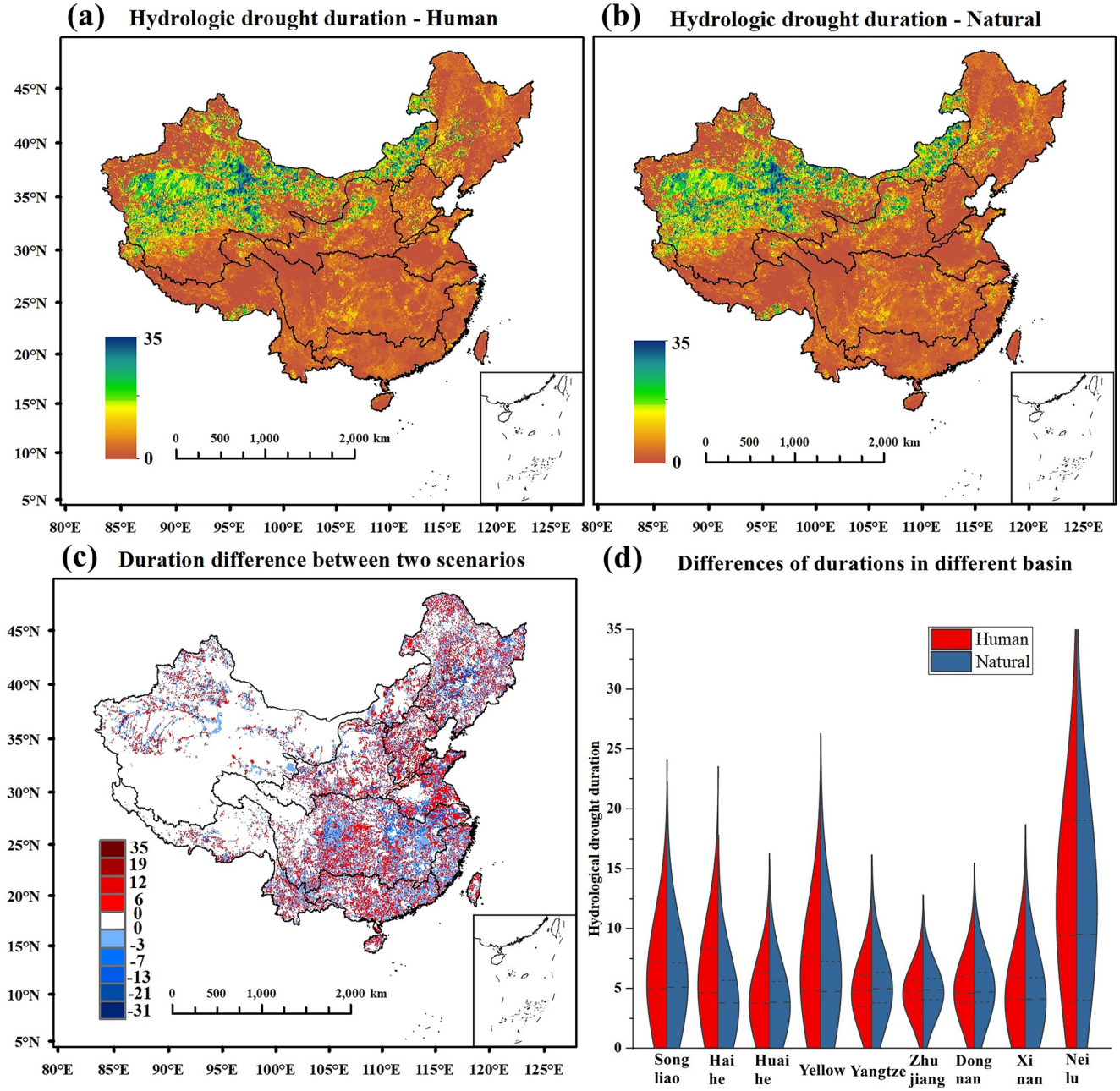

Figure 4. Spatial distribution of averaged hydrological drought duration (month) across China ((a) AnthrSim and (b) NatSim) and the difference between the two scenarios (human—natural) ((c) spatial distribution and (d) differences across sub-basins).

from the real-world situation, the PCR-GLOBWB v2.0 model still maintains a reasonable level of error when simulating human water usage.

4.1. The Impact of Human Activities on Hydrological Drought

The average drought duration shows spatial heterogeneity across China (Figure 4), with higher values in northwest China compared to the south under both scenarios (Figures 4a and 4b). The impact of human activities is mainly concentrated in the northeast, southeast, and central China, corresponding to an increase in drought duration (Figure 4c). In contrast, human activities reduced the drought duration by 1–7 months in parts of YZRB, DRB, ZRB and central SRB. This indicates that the impacts of human activities on hydrological drought duration are not consistent in the south and north of China.

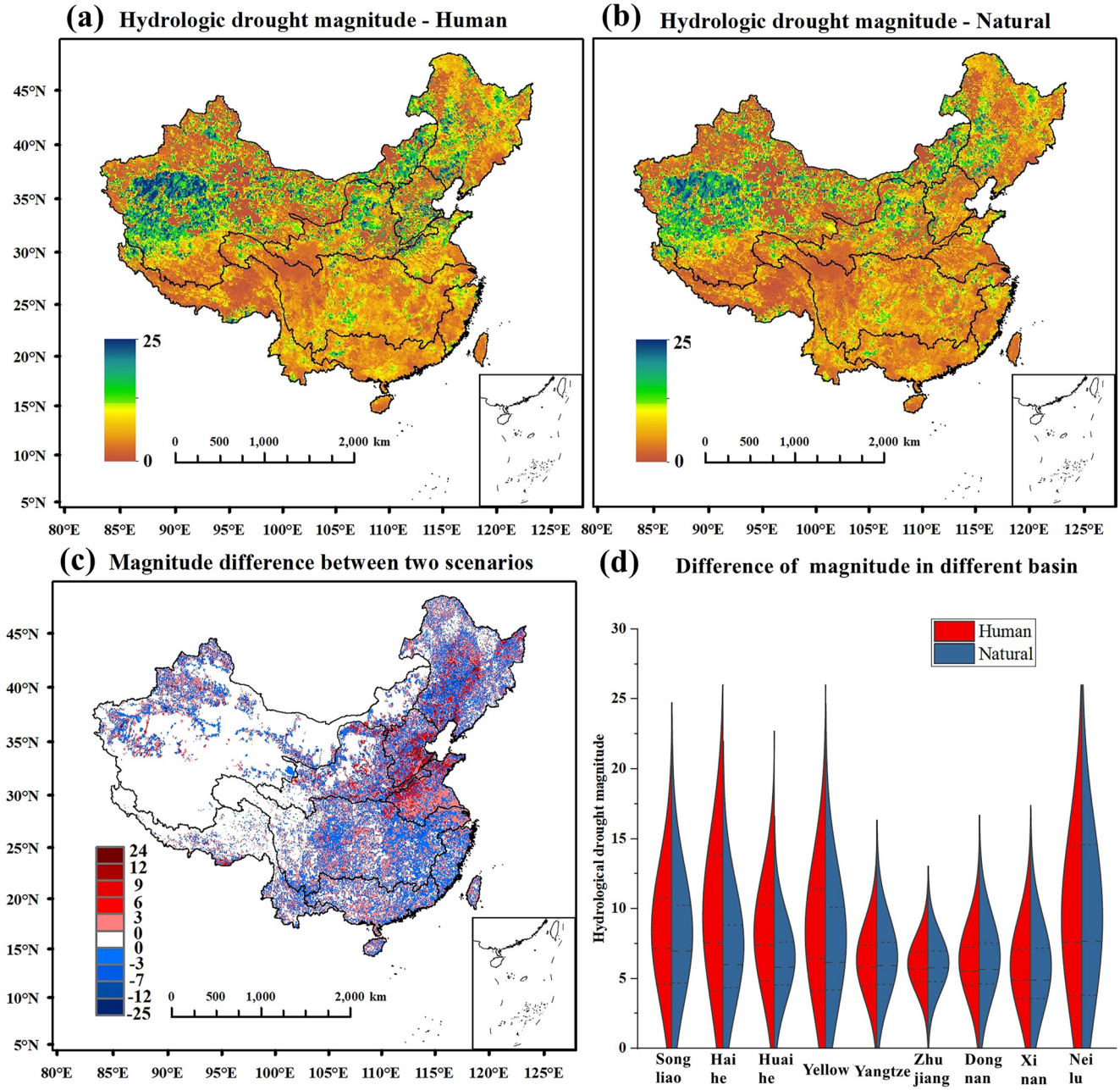

Figure 5. Same as Figure 4, but for the average hydrological drought magnitude.

Figure 5 shows the same information but for hydrological drought magnitude. The drought magnitude and duration show a similar spatial pattern, with an increasing gradient from the southeast coast to the northwest interior (Figures 5a and 5b). Drought magnitude under human activities is substantially higher in most areas of northern China. Especially in the HURB and HARB, the AnthrSim's drought magnitude increases by 1–2.5 on average (Figure 5d). The drought magnitude in southeast coastal China (lower YZRB, eastern ZRB, and DRB) has been alleviated by human activities, with a decrease between 0.1 and 7 (Figure 5c). These results demonstrate that human activities have opposite effects on drought magnitude in different basins.

Figure 6 shows the same analysis but for hydrological drought frequency, which shows less spatial variability as compared to duration and magnitude. Drought frequency ranges from 20 to 40 events, with a higher frequency in parts of northern China (Figures 6a and 6b). Within the areas affected by human activities, drought frequency

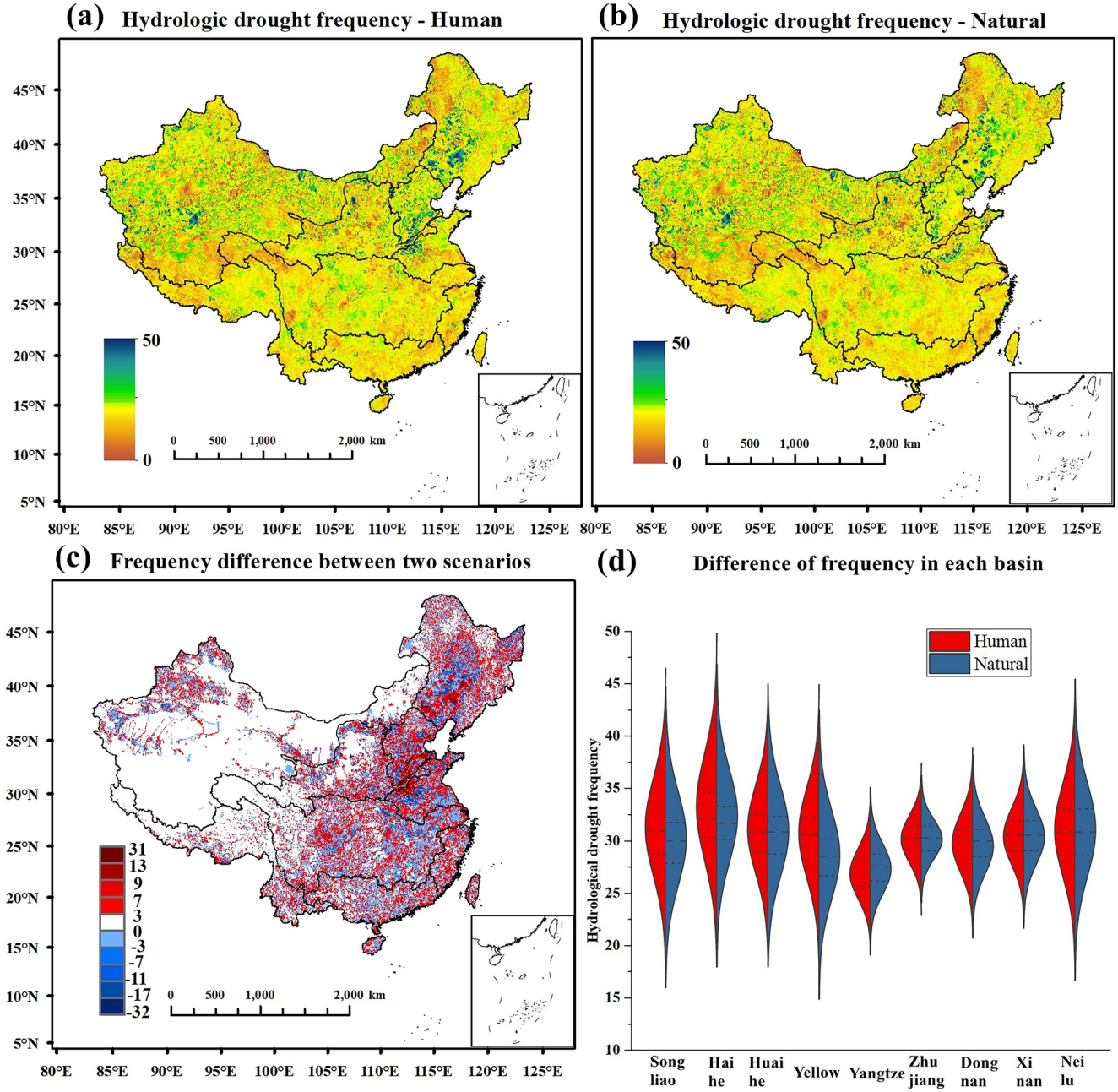

Figure 6. Same as Figure 4, but for the hydrological drought frequency (times).

increased by 3–31 in most basins, and decreased only in parts of YZRB and SRB (Figures 6c and 6d), by 1–32 events. Human activities (water extraction, irrigation, etc.) interfere with the natural terrestrial water cycle processes and impede the natural recharge of river systems, which is likely responsible for the general increase of drought frequency. Meanwhile, the decrease of drought duration, frequency and magnitude in the lower reaches of YZRB may be a benefit of reservoir regulation (e.g., Three Gorges Dam).

4.2. Influence of Human Activities on Drought Propagation Rate and Lag Time

The PR for the two scenarios and their differences are shown in Figures 7a and 7b. The PR ranged from 45% to 75% (Figure 7b), with lower PR in most parts of China affected by human activities. The regions where PR decreased substantially due to human activities were distributed in HARB and SRB, reaching a maximum 60% decrease (Figure 7a).

The PT is the maximum correlation between 1 and 24 months times scale SPI and SRI for the two scenarios (Figures 7c and 7d). The correlation coefficients of all basins (except NRB) are between 0.5 and 0.8, indicating a strong response of hydrological drought to meteorological drought. Under the influence of human activities, the correlation coefficients in HARB, HURB, YZRB, and YERB decreased at various levels (Figures 7c and 7d). Generally speaking, meteorological and hydrological droughts are strongly correlated in natural conditions, and human activities have weakened this relationship to some extent.

We took the time scale of SPI-n (n corresponding to the time scale with maximum correlation coefficient) as PT (Barker et al., 2016; Hellwig et al., 2020; Huang et al., 2019; Xu et al., 2019), and evaluated the differences of PT between two scenarios (Figures 7e and 7f). Overall, PT ranges from 6 to 23 months, with the PT in northern China generally longer than in the south (Figure 7f). As a result of human activities, the PT in SRB, YERB, HARB, and HURB was shortened by 1–13 months, while in DRB, ZRB, and lower YZRB, the PT was extended by 1–10 months (Figure 7e). Areas with substantial changes in PT correspond to intense human water extraction and irrigation activities (these areas are densely populated or have large irrigation districts).

PR decreased in most basins under human activities, ranging from 0.26% to 7.51%, with only slight increases in YZRB, YERB, and XRB (Figure 8a). The PR decreases more in the north than in the south, which may be due to the high human demand for water extraction and irrigation in northern China. Except in DRB and ZRB, the averaged PT decreases in all other basins (Figure 8b. Similar to the PR, the shortening of PT due to human activities is more substantial in northern China. It indicates that the effects of human activities are substantially different in southern and northern China.

4.3. Impact of Human Activities on Drought Propagation Characteristics in Typical Basins

The areas affected by human activities in terms of PT mainly include SRB, HARB, HURB, YERB, and YZRB (Figures 7e and 7f). In order to compare the propagation characteristics among different basins, we divided the basins into two groups according to the size of the basins. The first group is YZRB and YERB, and the second group is HARB and HURB. These basins are located in central China with a high magnitude of human activities, which is representative for reflecting human activities impact on drought propagation characteristics. SRB was not included because no suitable similar basins could be identified.

Based on the averaged PT in each basin, we determined the SPI time scale corresponding to SRI for the two scenarios (e.g., the AnthrSim SRI for the YERB corresponds to SPI-14). Following the method proposed by Barker et al. (2016), precipitation was spatially accumulated across the basin. Subsequently, the SPI-n was calculated and matched with the SRI extracted from the basin control stations. This process was carried out to obtain the corresponding drought events and their characteristics in the basin. (Figure S4 and Tables S2–S9 in Supporting Information S1). The scheme follows the physical mechanisms of flow generation and confluence. To further validate the feasibility of the proposed approach, correlation tests were performed on each basin separately (Figure S4 in Supporting Information S1). It can be observed that the SRI of each basin shows significant positive correlations with its corresponding SPI-n. This observation confirms the feasibility of the proposed approach.

The relationships between meteorological and hydrological drought characteristics were fitted using linear and non-linear models, and Table 1 gives the optimal fitting model (all fitting equations can be found in Table S10 in Supporting Information S1). The determination coefficients (R^2) of the fitted models are mostly above 0.8, indicating that the model fits well.

Figure S5 in Supporting Information S1 shows the fitted curves of the drought characteristics propagation for the YZRB and YERB. As the duration, magnitude, and recovery time of meteorological drought increase, the corresponding characteristics of hydrological drought also increase. The best-fit curves are given in Figure 9. When hydrological droughts last more than 25 months, the fitted curve for natural duration is above the AnthrSim's curve. This indicates that under the same meteorological drought conditions, the NatSim's hydrological drought duration is longer than in the AnthrSim. In the YZRB, the drought magnitude fitted curve for the NatSim is above the AnthrSim when $X > 15$, which implies that human activities have mitigated drought propagation to some extent. The NatSim's recovery time fitted curves are consistently lower than in the AnthrSim, indicating that the AnthrSim's hydrological drought recovery time is longer than in NatSim. The drought magnitude fitted curve for the AnthrSim in the YERB is slightly above the NatSim. The recovery time curve has an intersection point at $X = 8$, indicating that hydrological droughts recover more quickly when the duration is shorter than 8 months, while the opposite is true for longer than 8 months.

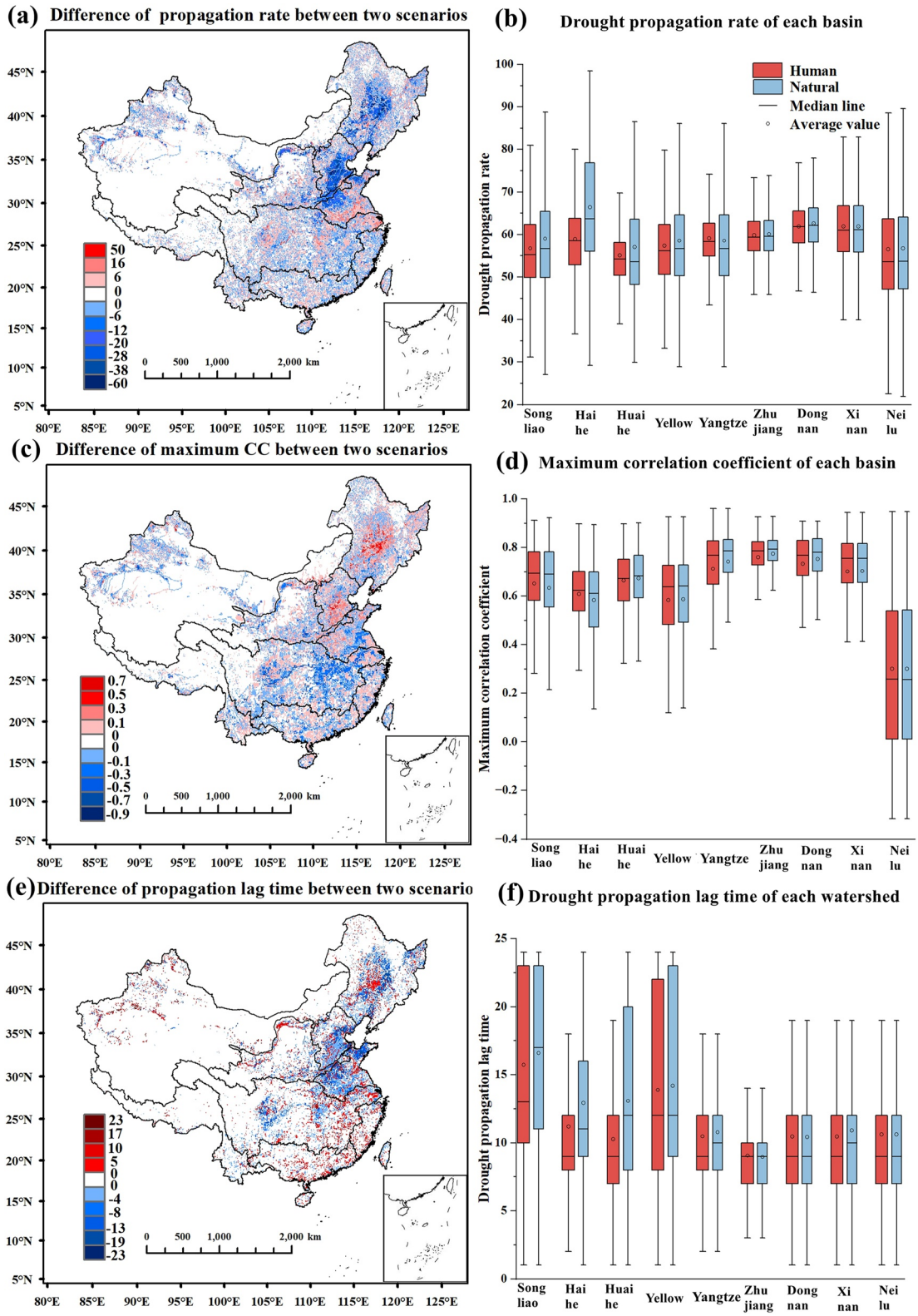

Figure 7. Spatial distribution of PR (a, b), maximum correlation coefficients (c, d), PT (e, f) and its differences (humn - natural) from meteorological drought propagation to hydrological drought under NatSim and AnthrSim in China.

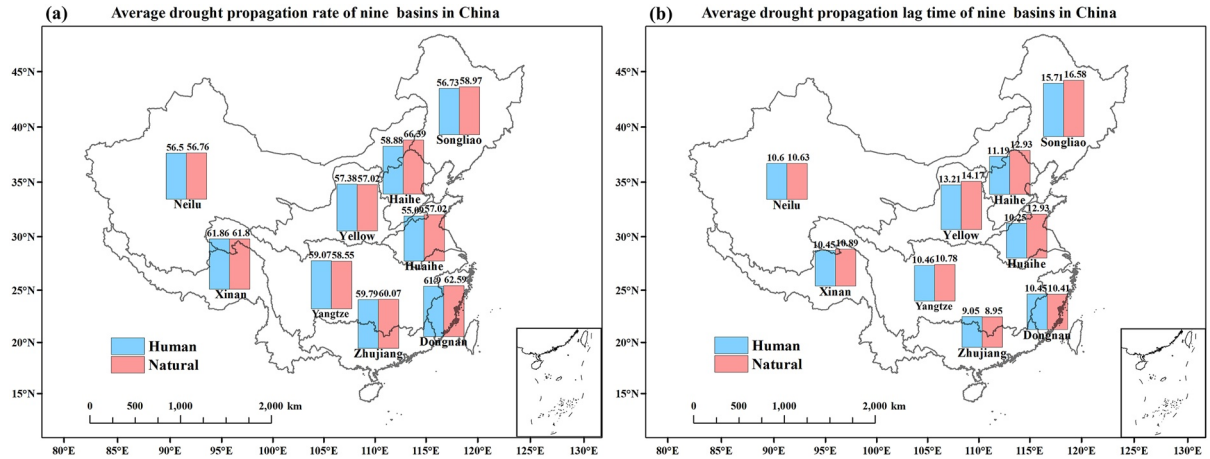

Figure 8. Averaged PR (a) and PT (b) for NatSim and AnthrSim in the nine basins of China.

Figure 10 shows the best-fit curves (Figure S6 in Supporting Information S1 provides all curves) of HURB and HARB. In the AnthrSim for HURB, the hydrological drought duration triggered by short-term meteorological drought (<10 months) is longer than in the NatSim. When $X > 20$, the hydrological drought magnitude is greater in the AnthrSim than in the NatSim. The recovery time propagation curves largely overlap. In HARB, for hydrological droughts triggered by meteorological droughts lasting longer than 12 months, the hydrological drought duration in the AnthrSim is always longer than in the NatSim. The hydrological drought magnitude in the AnthrSim is always larger than that in the NatSim.

Overall, the hydrological drought characteristics intensified in the northern basins (YERB, HARB) and the north-south divide basin (HURB). While, in the southern basin (YZRB), those characteristics were alleviated. In addition, we found that large basins were less affected by human activities than small ones, possibly because large basins have stronger self-regulation capabilities.

Table 1
Best-Fit Models of Drought Propagation Characteristics for Two Scenarios in Each Basin

	Human		Natural	
Drought characteristics	Fitting equation	R^2	Fitting equation	R^2
Yangtze River				
Duration	$y = 0.462 + 0.904x + 0.002x^2$	0.904	$y = \exp(1.068 + 0.133x - 0.001x^2)$	0.896
Magnitude	$y = \exp(4.479 - 41.214/(x + 10.503))$	0.948	$y = \exp(1.04 + 0.101x - 0.0006x^2)$	0.957
Recovery time	$y = 0.575 + 1.037x + 0.001x^2$	0.973	$y = x^{1.091}$	0.941
Yellow River				
Duration	$y = \exp(1.27 + 0.097x - 0.008x^2)$	0.905	$y = \exp(1.145 + 0.108x - 0.001x^2)$	0.883
Magnitude	$y = 1.503 + 0.567x + 0.014x^2$	0.929	$y = 1.72 + 0.573x + 0.013x^2$	0.835
Recovery time	$y = \exp(0.482 + 0.209x - 0.004x^2)$	0.745	$y = \exp(0.282 + 0.192x + 0.002x^2)$	0.907
Huaihe River				
Duration	$y = \exp(0.968 + 0.161x - 0.003x^2)$	0.736	$y = -0.191 + 0.945x + 0.0001x^2$	0.873
Magnitude	$y = -35.32 - 15.771\ln(x + 9.138)$	0.699	$y = -3.658 - 5.938\ln(x + 1.795)$	0.612
Recovery time	$y = \exp(0.130 + 0.355x - 0.015x^2)$	0.779	$y = \exp(0.057 + 0.341x - 0.012x^2)$	0.873
Haihe River				
Duration	$y = \exp(0.415 + 0.204x + 0.0035x^2)$	0.856	$y = \exp(0.746 + 0.168x - 0.002x^2)$	0.865
Magnitude	$y = \exp(0.553 + 0.134x - 0.001x^2)$	0.753	$y = -1.927 + 0.001(\text{abs}(x - 42.161)^{3.9})$	0.880
Recovery time	$y = \exp(0.682 + 0.138x + 0.001x^2)$	0.661	$y = 1.088 + 0.647x + 0.028x^2$	0.899

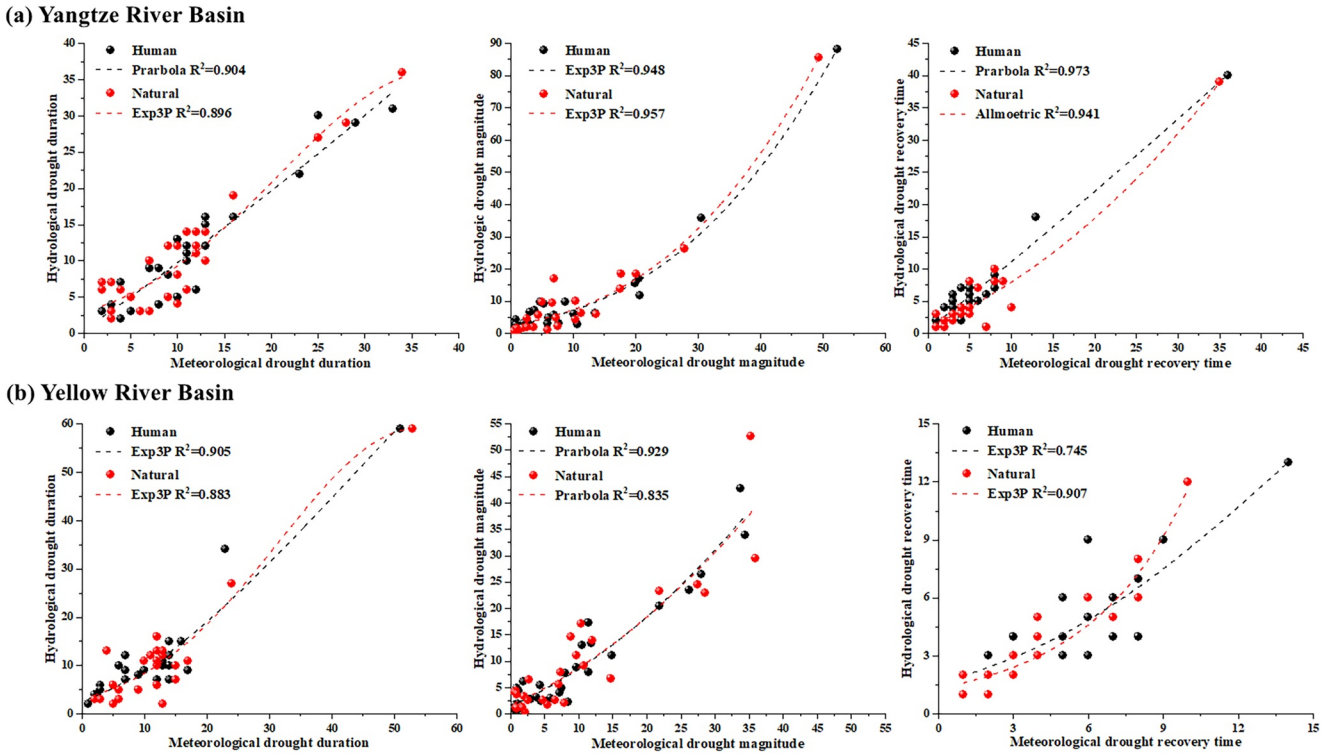

Figure 9. Best-fit curves for drought propagation characteristics in the YZRB (a) and YERB (b).

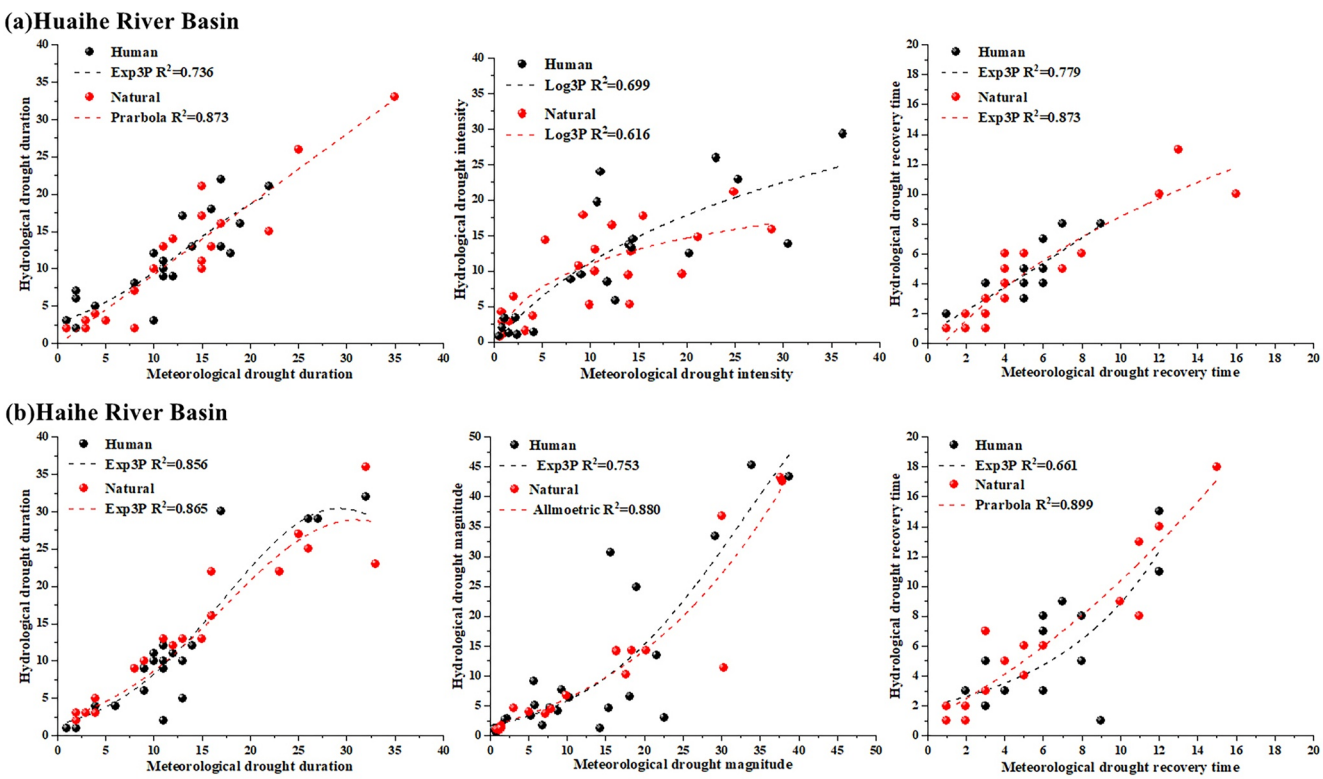

Figure 10. Best-fit response curves for drought characteristics propagation in the HURB (a) and HARB (b).

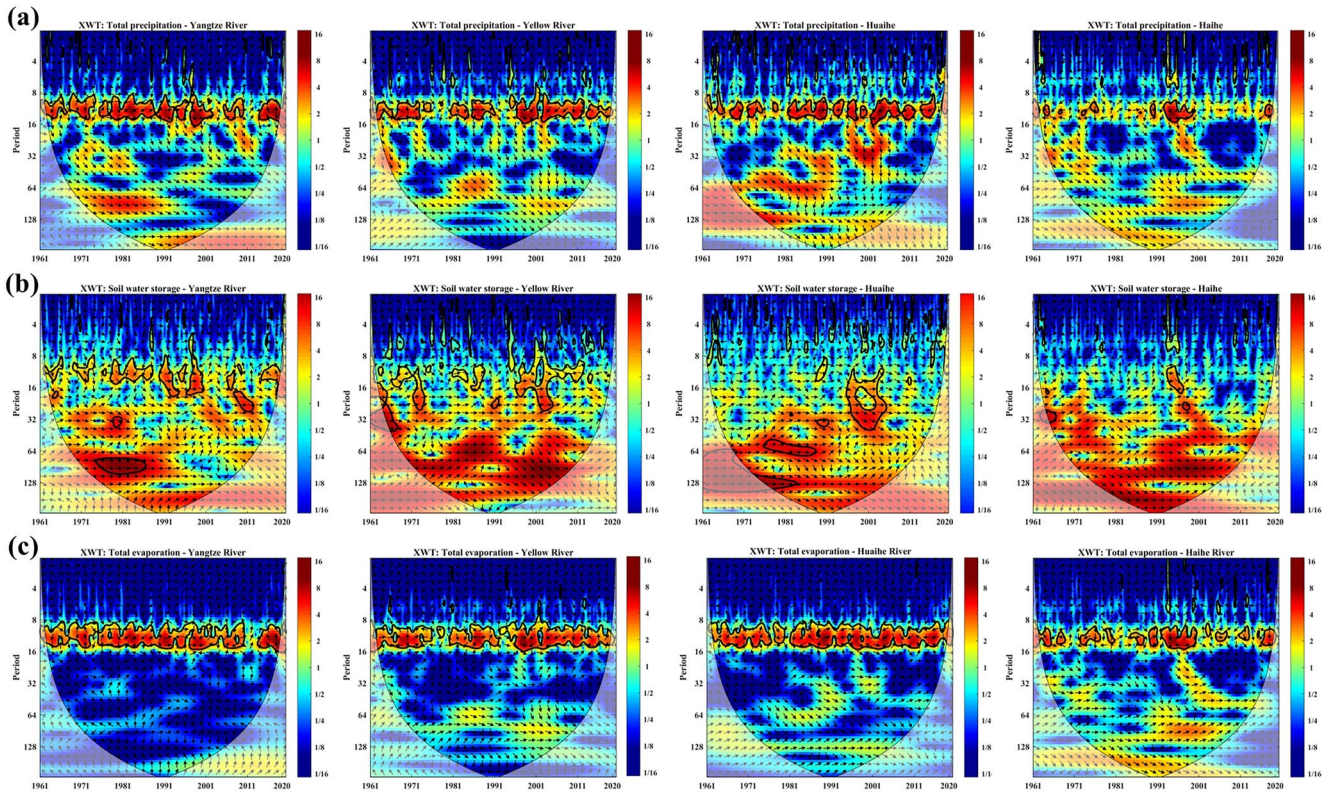

Figure 11. Cross wavelet transform spectra of SRI with influencing factors for the NatSim, (a) precipitation, (b) soil water, (c) total evaporation. Note: In the figure, the horizontal axis represents years, while the vertical axis represents time scales, which can also be understood as resonant periods. The shaded region enclosed by thick solid lines (mostly in deep red) indicates a passage through a 95% significance noise test, signifying significant correlation between the two signals at certain time scales. The direction of the arrows reflects their phase relationship: arrows pointing from left to right indicate positive correlation, while those pointing from right to left depict negative correlation between the two signals.

4.4. Association of Natural and Human Factors With Drought Propagation

We explored the association of potential influencing factors with drought propagation by the cross-wavelet transform. Figure 11 shows the cross-wavelet transform spectra of the natural factors with SRI. At 95% confidence level, there is a strong positive correlation between precipitation and SRI in the YERB, YZRB and HURB throughout the study period (arrows to the right), and a slightly weaker correlation in the HARB. The significantly correlated period of the wavelet spectrum is concentrated in 9–14 months (Figure 11a). The correlations between soil water content and SRI in the YERB and HARB are strong throughout the study period, while that in the YZRB and HURB are strong before 1990s and then weakened. Unlike precipitation, soil water content exhibited positive correlations concentrated in the 40–80 months period (Figure 11b). The high energy range of the evapotranspiration and SRI cross-wavelet spectra is similar to precipitation, and the period of high energy is concentrated in 9–14 months (Figure 11c). The wavelet periods of precipitation and evapotranspiration are generally consistent with the range of PT, and they both affect drought propagation in the short term (9–14 months). While, soil water content affects drought propagation via a slower process (40–80 months).

The relationship between the main human activity factors and drought propagation is shown in Figure 12. The high-energy period of irrigation water and SRI in the YZRB and YERB is mainly concentrated after the 1970s. This phenomenon occurred in the HURB and HARB after 1985, with a period of 9–14 months. This indicates that the YZRB and YERB carried out irrigation activities earlier and thus influenced hydrological drought (Figure 12a). In addition, there are long-period positive correlation areas in the HURB and HARB, which may be caused by the seepage of irrigation water to recharge soil water and groundwater. Groundwater abstraction and SRI shows a negative correlation (arrows to the left). After 1990, the contribution of groundwater abstraction to drought propagation was more pronounced in the HURB and HARB than before the 1990s. This relationship was weaker in the YERB and YZRB (Figure 12b). This implies that groundwater extraction in the HURB and HARB

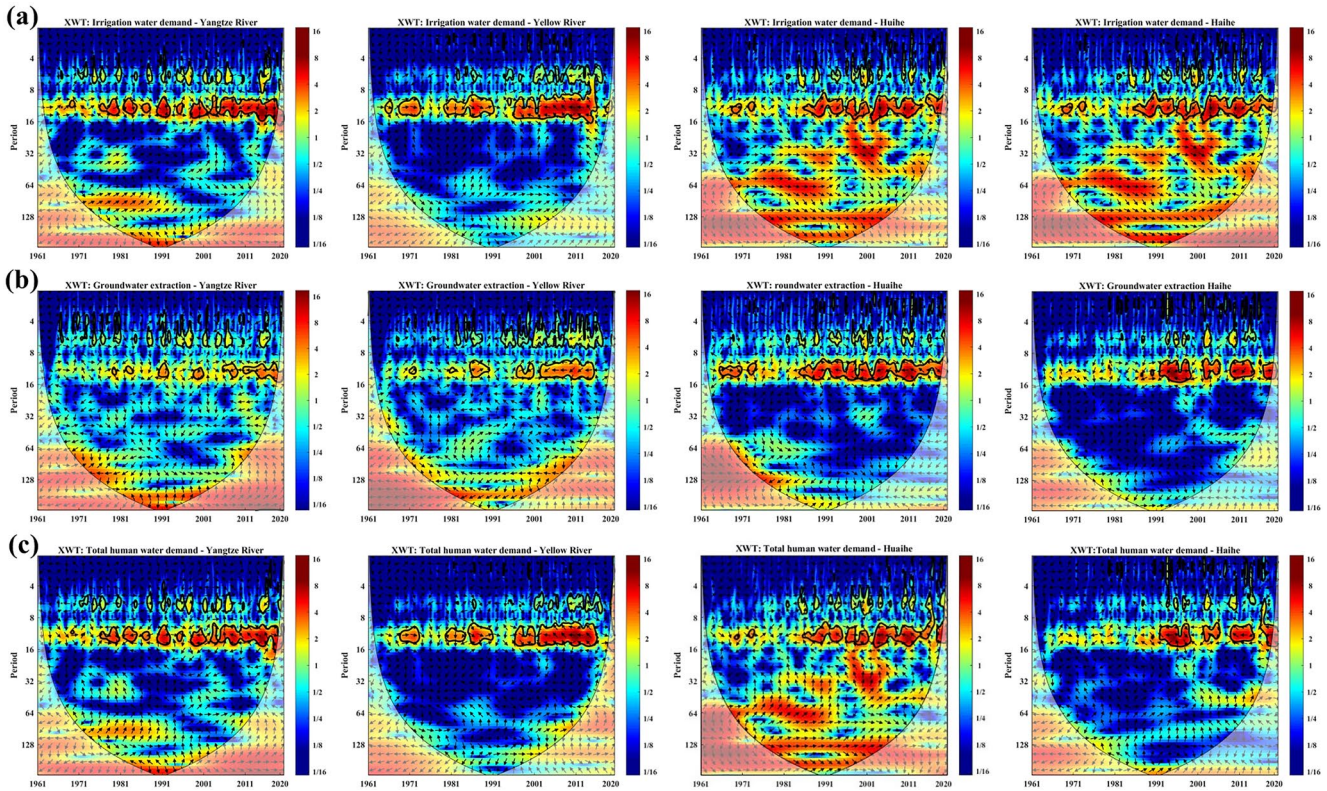

Figure 12. Cross wavelet transform spectra and influencing factors of SRI for the AnthrSim, (a) irrigation water, (b) groundwater abstraction, (c) human water demand.

has greatly affected the pattern of hydrological drought in recent years. Human water demand in the YZRB and YERB started to significantly influence drought propagation after the 1980s, and the relationship in the HURB and HARB started to be strong only after the 1990s (Figure 12c).

The impact of human and natural factors on drought propagation varies greatly. First, the influence of human factors on drought propagation has become stronger over the last three decades (Figure 12). While, natural factors have persistent impacts throughout the study period (Figure 11). Second, the influence of human factors on SRI is mainly concentrated in 9–14 months (Figure 12), while the influence of some natural factors can reach 40–80 months (Figure 11). Finally, all human activity factors were negatively correlated with SRI, suggesting that human water withdrawal exacerbates drought. In addition, the roles played by these factors in the process of drought propagation exhibit significant spatial variations.

5. Discussion

5.1. Mechanism of Human Activities Affect Hydrological Drought and Drought Propagation

Human activities have altered the patterns of hydrological drought and its propagation in China. Human production and daily water use, including domestic, industrial, and livestock water use, are relatively evenly distributed throughout the year and have a high return rate (Van Beek et al., 2011; Van Loon & Laaha, 2015; Wada et al., 2013). In contrast, irrigation, usually carried out during the dry season in water-scarce regions (X. Liu et al., 2019), is considered the primary factor exacerbating hydrological drought in China (Shao et al., 2018; Yang et al., 2020). Taking the Yellow River Basin as an example, we separately calculated the magnitude of hydrological drought under the activation of the irrigation/human water use and reservoir modules (Figure S7 in Supporting Information S1). Then, the differences between them and NatSim were compared. It can be seen that, compared to other factors, irrigation is the primary factor exacerbating hydrological droughts.

To reveal the mechanisms by which irrigation activities affect hydrological drought and its propagation in China, we extracted and compared some irrigation-related factors (Figure 13).

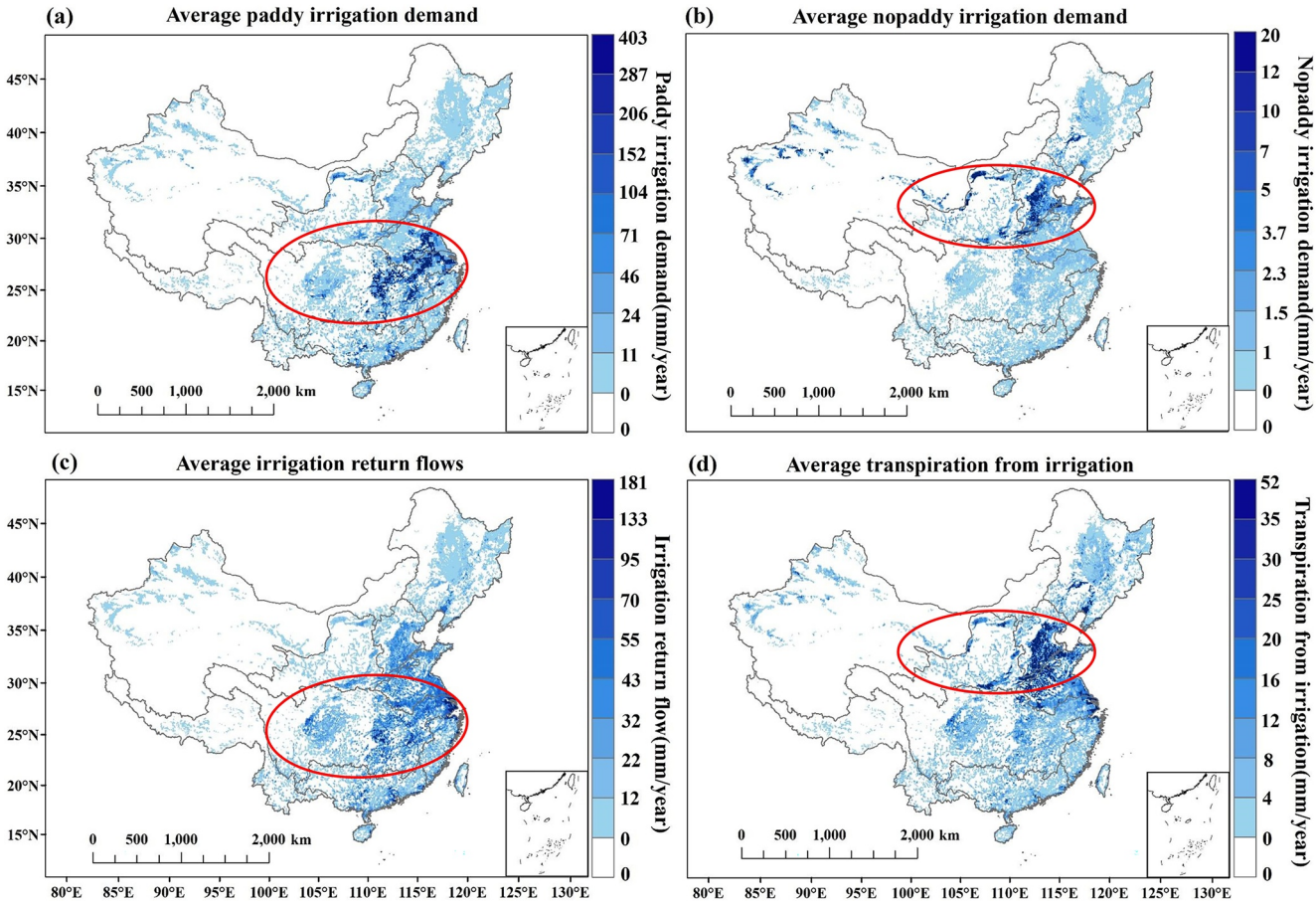

Figure 13. Average annual distribution of irrigation factors: (a) paddy irrigation demand, (b) nopaddy irrigation demand, (c) irrigation return flow, (d) crop transpiration from irrigation.

The proportion of irrigation water to total water intake varies greatly between northern and southern China. According to statistics from the Yellow River Conservancy Commission (YRCC, http://www.yrcc.gov.cn/), irrigation water in the Yellow River basin accounts for about 60% of total water intake. In the south, due to abundant surface water resources, the proportion of water extracted for irrigation is smaller, for example, in the Yangtze River basin this proportion is about 35% (Changjiang Water Resources Commission, CWRC, http://www.cjw.gov.cn/). This conclusion has been confirmed by previous research results (Dai et al., 2008; Liu et al., 2017; Wada et al., 2013). In addition, irrigation water in the Yellow River basin accounts for 80%–90% of the total reduced flow of the Yellow River, which may be the main cause of hydrological drought intensification (Wang, 1998).

There are significant differences in irrigation patterns between northern and southern China, with paddy irrigation concentrated in the south (Figure 13a), while the water demand for nopaddy irrigation is greater in the north (Figure 13b). Different irrigation patterns have a significant impact on hydrological drought. Due to the water storage required in fields during the growth season of paddy irrigation, the water will seep into the soil and return to groundwater or rivers through infiltration and soil flow (Leng & Tang, 2014; Liu et al., 2005), resulting in little water loss. Therefore, the irrigation return flow in southern China is greater than in the north (Figure 13c). The greater transpiration of crops is also one of the driving factors exacerbating water scarcity in northern China (Figure 13d). Chen et al. (2003) showed that high transpiration in northern irrigation areas results in a large amount of surface and groundwater loss, reducing the proportion of irrigation return flow and exacerbating local hydrological drought.

The impact of the regulation function of reservoirs on hydrological drought cannot be ignored. In southern China, where water resources are abundant, a large amount of water is collected during flood season. The existence of reservoirs reduces the surplus water during this period and stores it to alleviate water scarcity during drought

season (Dai et al., 2008; Shao et al., 2018; Wang et al., 2017; Yuan et al., 2017). The multi-year average storage capacity of reservoirs in southern China is much higher than that in the north (Figure S8 in Supporting Information S1). Taking the Yangtze River as an example, according to statistics from CWRC, the annual average storage capacity in the basin is about 1350×10^8 m^3. During the severe drought in 2011, the Three Gorges Dam released approximately 215×10^8 m^3 of water to alleviate the situation. However, there are relatively fewer reservoirs in northern China compared to the south, and water resources are relatively scarce. As a result, the amount of water stored during the non-drought season is relatively small. Irrigation activities in these areas during the crop growing season mainly rely on water supply from reservoirs. When a drought occurs, the reservoirs do not have enough storage capacity to alleviate it (X. Liu et al., 2019), resulting in an exacerbation of the drought situation.

We found an interesting phenomenon that the PR/PT of most basins under the AnthrSim are decreased/shortened compared with the NatSim (Figures 6b and 6f). The main reason for the decline of PR may be the implementation of various drought-resistance measures, such as various water management projects, including reservoir management and storage, etc. When meteorological drought occurred, water management caused the connection between the meteorological drought and the hydrological drought to be curtailed, and the hydrological drought that should have occurred naturally was effectively controlled, in agreement with Wan et al. (2017). Such drought-resistance measures have led to a reduction in the number of hydrological drought events associated with meteorological drought, resulting in a substantial decrease in PR. Over the past 30 years, increased irrigation and water demand, as well as high-intensity groundwater withdrawals have disrupted the natural water cycle, disrupting the natural recharge of rivers and accelerating the development of hydrological droughts (Ma et al., 2019), resulting in a shortening of the PT. This phenomenon is more pronounced in the northern basins (SRB, HARB, HURB, YERB). The decline/shortening of PR/PT in these areas may be related to water scarcity and over-exploitation in northern China, where increased water stress further affects hydrological drought. While, the abundant water resources and water management measures (reservoir regulation) in southern China have mitigated the impact caused by human activities to some extent.

5.2. Uncertainty From Meteorological Forcing and Model

Meteorological forcing is crucial for hydrological modeling but can also introduce uncertainty (Chilkoti et al., 2017; Wang et al., 2017; Wei et al., 2020). We examined the uncertainty introduced by interpolation methods by randomly selecting 85% of the stations for interpolation and using the remaining 15% for accuracy validation (Figure S9 in Supporting Information S1). Linear trends for most meteorological variables at the stations were good, with precipitation biases ranging from −10% to 7.5% and temperature biases between −1°C and 2°C, indicating that the uncertainty from the interpolation methods remains within reasonable bounds. However, in regions with low meteorological station coverage, especially in NRB, the representativeness of the model can be compromised. This implies that meteorological variables in large areas not covered by station networks need to rely on estimation, which will increase uncertainty and, consequently, impact the accuracy and reliability of hydrological simulations (Barman et al., 2014). Future work should aim to acquire more observational data or utilize satellite remote sensing data to fill the gaps in the meteorological station network, providing a more comprehensive meteorological data set (Wei et al., 2022; Yu et al., 2023).

We used the Yangtze River and Yellow River basins as typical cases to estimate the impact of incorporating human activities into the model on streamflow simulations. The Nash-Sutcliffe Efficiency (NSE) between the observed and NatSim/AnthrSim simulated streamflow are calculated in Table S11 in Supporting Information S1. It showed that simulated streamflow considering human influence perform better than those under natural conditions. While including human activities enhances the performance of streamflow simulations (Sutanudjaja et al., 2018), the model is reliant on the accuracy of human water consumption calculations (De Graaf et al., 2014; Wada et al., 2013). This study compared annual human water deviations between statistical data and model's simulations (Figure S3 in Supporting Information S1) for approximate human impacts in region scale. Meanwhile, the evaluations at an annual scale cannot capture the seasonality of human water withdrawal and irrigation (Cheng et al., 2021). These uncertainties may overestimate/underestimate the human water withdrawals, results in estimation biaes of flow reduction effects and introduce biases into the assessment of drought conditions (Wang et al., 2020; Zhang et al., 2022).

To validate the impact of the inherent uncertainty in the model simulation, we extracted the model database over China from the global database of the PCR-GLOBWB model (available through the ISIMIP intercomparison

project) (Sutanudjaja et al., 2018) and used it to calculate the SRI for comparison with our study (Figure S10 in Supporting Information S1). The differences in most regions are generally within the range of −0.2 to 0.2, with slightly larger discrepancies only found on the western of the Qinghai-Tibet Plateau and edge of SRB. The meteorological stations in these areas are very scattered, and errors driven by meteorological factors may be the cause of inconsistencies in hydrological simulations. Both data sets reflect similar drought conditions, indicating that the uncertainty in our drought estimation results is within a reasonable range. Nevertheless, there are uncertainties in the model's structure and parameters. First, the model does not account for inter-basin water diversion plans (Wada et al., 2016), such as China's renowned South-to-North Water Diversion Project, which provides some relief to water-deficient regions during dry seasons. Consequently, in the model, water resource demands in water-scarce areas can only be met locally, potentially leading to an overestimation of water extraction and, consequently, an overestimation of drought severity in these regions (Wada et al., 2016). Second, the parameters were extracted from a global database without local calibration. These uncertainties can result in deviations between model simulations and actual conditions (Shah et al., 2021; Van Loon et al., 2019).

5.3. Limitations of the Study

The PCR-GLOBWB v2.0 model represents multiple human activity processes, and this study confirms its reliability in simulating the effects of anthropogenic activities on hydrological processes. However, there are still some limitations. This study primarily focuses on the impact of human water withdrawal, irrigation, and reservoir regulation on hydrological drought, without taking into account the role of changes in land cover types. While we have isolated the effect of irrigation and other water management strategies, addressing this issue is left for further study. In addition, we used a standardized drought index and set the threshold at −0.5 to identify drought events. This threshold has the advantage of capturing the onset, development, and decline of all drought events effectively. However, different threshold choices may influence the results. For instance, lowering the threshold to −1 or −1.5 could lead to variations in the characteristics of drought events and the outcomes of propagation models. In the future, further subdivision of drought level should be considered to comprehensively explore their characteristics and propagation patterns. The drought response model considers all drought events, and its reliability in fitting drought characteristics has been confirmed by multiple studies (Huang et al., 2021; Wu et al., 2017, 2021). Whereas, the choice of fitting functions can sometimes be influenced by one or several major drought events, leading to uncertainty. We should consider adopting more methods capable of handling complex dependency relationships, such as using Copula functions to describe the nonlinear relationships between drought propagation in the future researches. Furthermore, the research framework of this paper can only reveal the extent of human activities on drought propagation, while the mechanism of human activities affecting drought propagation is not fully addressed, indicating that future research should focus on such topics.

6. Conclusion

We used the PCR-GLOBWB v2.0 model to simulate the terrestrial water cycle in China (1961–2020) under NatSim and AnthrSim, distinguishing the degree of human impacts on hydrological drought and drought propagation. The following conclusions were obtained.

1. The impact of human activities is mainly concentrated in the northeastern, southern and central China, reducing the severity of hydrological drought in the south, but exacerbating it in the north. The averaged hydrological drought duration in most of northern China was extended by 1–12 months, the magnitude increased by 0–9, and the frequency increased by 3–31 events. In contrast, in parts of the YZRB and the DRB, the average drought duration was shortened by 1–7 months, the magnitude was reduced by 0–7, and frequency was reduced by 1–32 events.
2. The PR of meteorological to hydrological drought in China is 45%–75%, with little variability from north to south. The PT ranges from 6 to 23 months, and it is generally longer in the north than south. The response rate decreased by 1%–60% in most areas of China due to human activities, and the substantial decreases were distributed in the HARB and SRB. Human activities have led to 1–13 months reduction in PT in the SRB, YERB, HARB, HURB, and 1–10 months extension in parts of the DRB, ZRB, and Lower YZRB.
3. The nonlinear model fits better to the meteorlogical and hydrological drought characteristics than the linear model, with most of determination coefficients R^2 above 0.8. It indicates that the reliability of the fitted model. As the duration, magnitude and recovery time of meteorological drought increased, the corresponding

characteristics of hydrological drought also increased. Under the same meteorological drought conditions, human activities exacerbated/mitigated drought propagation characteristics in the northern/southern basins, respectively. In addition, the larger basins were less affected by human activities than the smaller basins.

4. The correlation between natural factors and drought propagation is high throughout the study period, with precipitation and evapotranspiration having a short period of influence (9–14 months). While, soil water content slowly (40–80 months) influences drought propagation. The impact of human factors has become more pronounced in the last three decades, all showing negative correlations, indicating that human water extraction generally exacerbates hydrological drought.

Data Availability Statement

The PCR-GLOBWB v2.0 model code, model parameters and their components used in the paper are provided by the Github repository (https://github.com/UU-Hydro/PCR-GLOBWB_model). The input files of the model is stored on the following website (https://zenodo.org/records/1045339). The ini-files used to configure the parameter files and invoke the model are stored on the following website (https://github.com/UU-Hydro/PCR-GLOBWB_model/tree/master/clone_landmask_maps) The global output results of the model can be obtained from the following website (https://opendap.4tu.nl/thredds/catalog/data2/pcrglobwb/catalog.html). The file for configuring the model runtime environment (https://github.com/UU-Hydro/PCR-GLOBWB_model/blob/master/conda_env/pcrglobwb_py3.yml). Meteorological data are available at China Meteorological Data Service Center (http://data.cma.cn/). The water usage statistics of various provinces in China are sourced from the Water Resources Bulletin (http://www.mwr.gov.cn/). Data of abstraction water from groundwater and surface water, irrigation water and irrigation return water, and storage capacity of all reservoirs in Yellow River and Yangtze River were collected from the water resources bulletins of the Yellow River and Yangtze River, which can be downloaded from Yellow River Conservancy Commission (YRCC, http://www.yrcc.gov.cn/zwzc/gzgb/gb/szygb/) and Changjiang Water Resources Commission (CWRC, http://www.cjw.gov.cn/zwzc/bmgb/).

Acknowledgments

This work was supported by the National Natural Science Foundation of China (Grants. U2243203 and 52079036), the Fundamental Research Funds for the Central Universities (Grants B220201011), and the Natural Science Foundation of Jiangsu Province (Grant BK20210368). The authors are grateful to the Editor and anonymous reviewers for their constructive comments. This study complies with the AGU data policy.

References

AghaKouchak, A., Feldman, D., Hoerling, M., Huxman, T., & Lund, J. (2015). Water and climate: Recognize anthropogenic drought. *Nature*, *524*(7566), 409–411. https://doi.org/10.1038/524409a

American Meteorological Society. (1997). Meteorological drought-policy statement. *Bulletin America Meteorology Social*, *78*, 847–849.

Apurv, T., Sivapalan, M., & Cai, X. (2017). Understanding the role of climate characteristics in drought propagation. *Water Resources Research*, *53*(11), 9304–9329. https://doi.org/10.1002/2017wr021445

Barker, L. J., Hannaford, J., Chiverton, A., & Svensson, C. (2016). From meteorological to hydrological drought using standardized indicators. *Hydrology and Earth System Sciences*, *20*(6), 2483–2505. https://doi.org/10.5194/hess-20-2483-2016

Barman, R., Jain, A. K., & Liang, M. (2014). Climate-driven uncertainties in modeling terrestrial gross primary production: A site level to global-scale analysis. *Global Change Biology*, *20*(5), 1394–1411. https://doi.org/10.1111/gcb.12474

Bierkens, M. F., Bell, V. A., Burek, P., Chaney, N., Condon, L. E., David, C. H., et al. (2015). Hyper-resolution global hydrological modelling: What is next? "Everywhere and locally relevant". *Hydrological Processes*, *29*(2), 310–320. https://doi.org/10.1002/hyp.10391

Chen, J., He, D., & Cui, S. (2003). The response of river water quality and quantity to the development of irrigated agriculture in the last 4 decades in the Yellow River Basin, China. *Water Resources Research*, *39*(3), 1047. https://doi.org/10.1029/2001wr001234

Cheng, H., Wang, W., van Oel, P. R., Lu, J., Wang, G., & Wang, H. (2021). Impacts of different human activities on hydrological drought in the Huaihe River Basin based on scenario comparison. *Journal of Hydrology: Regional Studies*, *37*, 100909. https://doi.org/10.1016/j.ejrh.2021.100909

Chilkoti, V., Bolisetti, T., & Balachandar, R. (2017). Climate change impact assessment on hydropower generation using multi-model climate ensemble. *Renewable Energy*, *109*, 510–517. https://doi.org/10.1016/j.renene.2017.02.041

Dai, Z., Du, J., Li, J., Li, W., & Chen, J. (2008). Runoff characteristics of the Changjiang River during 2006: Effect of extreme drought and the impounding of the three Gorges Dam. *Geophysical Research Letters*, *35*(7), L07406. https://doi.org/10.1029/2008gl033456

De Graaf, I. E., Gleeson, T., Sutanudjaja, E. H., & Bierkens, M. F. (2019). Environmental flow limits to global groundwater pumping. *Nature*, *574*(7776), 90–94. https://doi.org/10.1038/s41586-019-1594-4

De Graaf, I. E. M., Van Beek, L. P. H., Wada, Y., & Bierkens, M. F. P. (2014). Dynamic attribution of global water demand to surface water and groundwater resources: Effects of abstractions and return flows on river discharges. *Advances in Water Resources*, *64*, 21–33. https://doi.org/10.1016/j.advwatres.2013.12.002

Faiz, M. A., Liu, D., Fu, Q., Sun, Q., Li, M., Baig, F., et al. (2018). How accurate are the performances of gridded precipitation data products over Northeast China? *Atmospheric Research*, *211*, 12–20. https://doi.org/10.1016/j.atmosres.2018.05.006

FAO, F. (2018). The impact of disasters and crises on agriculture and food security. Report.

Food and Agriculture Organization of the United Nations (FAO). (2003). Digital soil map of the world, version 3.6. Retrieved from http://www.fao.org/nr/land/soils/digital-soil-map-of-the-world

Food and Agriculture Organization of the United Nations (FAO). (2007). *Gridded livestock of the world 2007*. In G. R. W. Wint & T. P. Robinson (Eds.), (pp. 131). Retrieved from http://www.fao.org/docrep/010/a1259e/a1259e00

Food and Agriculture Organization of the United Nations (FAO). (2016). AQUASTAT database of waterrelated data. Retrieved from http://www.fao.org/nr/water/aquastat/main/index.stm

Guo, Y., Huang, S., Huang, Q., Leng, G., Fang, W., Wang, L., & Wang, H. (2020). Propagation thresholds of meteorological drought for triggering hydrological drought at various levels. *Science of the Total Environment*, *712*, 136502. https://doi.org/10.1016/j.scitotenv.2020.136502
Gupta, H. V., Kling, H., Yilmaz, K. K., & Martinez, G. F. (2009). Decomposition of the mean squared error and NSE performance criteria: Implications for improving hydrological modelling. *Journal of Hydrology*, *377*(1–2), 80–91. https://doi.org/10.1016/j.jhydrol.2009.08.003
Han, Z., Huang, S., Huang, Q., Leng, G., Wang, H., Bai, Q., et al. (2019). Propagation dynamics from meteorological to groundwater drought and their possible influence factors. *Journal of Hydrology*, *578*, 124102. https://doi.org/10.1016/j.jhydrol.2019.124102
He, X., Estes, L., Konar, M., Tian, D., Anghileri, D., Baylis, K., et al. (2019). Integrated approaches to understanding and reducing drought impact on food security across scales. *Current Opinion in Environmental Sustainability*, *40*, 43–54. https://doi.org/10.1016/j.cosust.2019.09.006
He, X., Pan, M., Wei, Z., Wood, E. F., & Sheffield, J. (2020). A global drought and flood catalogue from 1950 to 2016. *Bulletin of the American Meteorological Society*, *101*(5), E508–E535. https://doi.org/10.1175/bams-d-18-0269.1
He, X., & Sheffield, J. (2020). Lagged compound occurrence of droughts and pluvials globally over the past seven decades. *Geophysical Research Letters*, *47*(14), e2020GL087924. https://doi.org/10.1029/2020gl087924
He, X., Wada, Y., Wanders, N., & Sheffield, J. (2017). Intensification of hydrological drought in California by human water management. *Geophysical Research Letters*, *44*(4), 1777–1785. https://doi.org/10.1002/2016gl071665
Hellwig, J., de Graaf, I. E. M., Weiler, M., & Stahl, K. (2020). Large-scale assessment of delayed groundwater responses to drought. *Water Resources Research*, *56*(2), e2019WR025441. https://doi.org/10.1029/2019wr025441
Herrera-Estrada, J. E., Satoh, Y., & Sheffield, J. (2017). Spatiotemporal dynamics of global drought. *Geophysical Research Letters*, *44*(5), 2254–2263. https://doi.org/10.1002/2016gl071768
Huang, S., Huang, Q., Chang, J., Leng, G., & Xing, L. (2015). The response of agricultural drought to meteorological drought and the influencing factors: A case study in the Wei River Basin, China. *Agricultural Water Management*, *159*, 45–54. https://doi.org/10.1016/j.agwat.2015.05.023
Huang, S., Li, P., Huang, Q., Leng, G., Hou, B., & Ma, L. (2017). The propagation from meteorological to hydrological drought and its potential influence factors. *Journal of Hydrology*, *547*, 184–195. https://doi.org/10.1016/j.jhydrol.2017.01.041
Huang, S., Wang, L., Wang, H., Huang, Q., Leng, G., Fang, W., & Zhang, Y. (2019). Spatio-temporal characteristics of drought structure across China using an integrated drought index. *Agricultural Water Management*, *218*, 182–192. https://doi.org/10.1016/j.agwat.2019.03.053
Huang, S., Zhang, X., Chen, N., Li, B., Ma, H., Xu, L., et al. (2021). Drought propagation modification after the construction of the three Gorges Dam in the Yangtze River Basin. *Journal of Hydrology*, *603*, 127138. https://doi.org/10.1016/j.jhydrol.2021.127138
Hudgins, L., Friehe, C. A., & Mayer, M. E. (1993). Wavelet transforms and atmospheric turbulence. *Physical Review Letters*, *71*(20), 3279–3282. https://doi.org/10.1103/physrevlett.71.3279
Hunt, E. D., Svoboda, M., Wardlow, B., Hubbard, K., Hayes, M., & Arkebauer, T. (2014). Monitoring the effects of rapid onset of drought on non-irrigated maize with agronomic data and climate-based drought indices. *Agricultural and Forest Meteorology*, *191*, 1–11. https://doi.org/10.1016/j.agrformet.2014.02.001
Jiang, S., Wang, M., Ren, L., Xu, C. Y., Yuan, F., Liu, Y., et al. (2019). A framework for quantifying the impacts of climate change and human activities on hydrological drought in a semiarid basin of Northern China. *Hydrological Processes*, *33*(7), 1075–1088. https://doi.org/10.1002/hyp.13386
Jiao, D., Wang, D., & Lv, H. (2020). Effects of human activities on hydrological drought patterns in the Yangtze River Basin, China. *Natural Hazards*, *104*(1), 1111–1124. https://doi.org/10.1007/s11069-020-04206-2
Jin, D., Guan, Z., & Tang, W. (2013). The extreme drought event during winter–spring of 2011 in East China: Combined influences of teleconnection in midhigh latitudes and thermal forcing in Maritime Continent region. *Journal of Climate*, *26*(20), 8210–8222. https://doi.org/10.1175/jcli-d-12-00652.1
Kao, S. C., & Govindaraju, R. S. (2010). A copula-based joint deficit index for droughts. *Journal of Hydrology*, *380*(1–2), 121–134. https://doi.org/10.1016/j.jhydrol.2009.10.029
Kling, H., Fuchs, M., & Paulin, M. (2012). Runoff conditions in the upper Danube basin under an ensemble of climate change scenarios. *Journal of Hydrology*, *424*, 264–277. https://doi.org/10.1016/j.jhydrol.2012.01.011
Leng, G. Y., & Tang, Q. H. (2014). Modeling the impacts of future climate change on irrigation over China: Sensitivity to adjusted projections. *Journal of Hydrometeorology*, *15*(5), 2085–2103. https://doi.org/10.1175/jhm-d-13-0182.1
Li, Q., Zhou, J., Zou, W., Zhao, X., Huang, P., Wang, L., et al. (2021). A tributary-comparison method to quantify the human influence on hydrological drought. *Journal of Hydrology*, *595*, 125652. https://doi.org/10.1016/j.jhydrol.2020.125652
Liu, J., Liu, M., Tian, H., Zhuang, D., Zhang, Z., Zhang, W., et al. (2005). Spatial and temporal patterns of China's cropland during 1990–2000: An analysis based on Landsat TM data. *Remote Sensing of Environment*, *98*(4), 442–456. https://doi.org/10.1016/j.rse.2005.08.012
Liu, S., Huang, S., Xie, Y., Huang, Q., Wang, H., & Leng, G. (2019). Assessing the non-stationarity of low flows and their scale-dependent relationships with climate and human forcing. *Science of the Total Environment*, *687*, 244–256. https://doi.org/10.1016/j.scitotenv.2019.06.025
Liu, X., Liu, W., Yang, H., Tang, Q., Flörke, M., Masaki, Y., et al. (2019). Multimodel assessments of human and climate impacts on mean annual streamflow in China. *Hydrology and Earth System Sciences*, *23*(3), 1245–1261. https://doi.org/10.5194/hess-23-1245-2019
Liu, X., Tang, Q., Cui, H., Mu, M., Gerten, D., Gosling, S. N., et al. (2017). Multimodel uncertainty changes in simulated river flows induced by human impact parameterizations. *Environmental Research Letters*, *12*(2), 025009. https://doi.org/10.1088/1748-9326/aa5a3a
Logan, K. E., Brunsell, N. A., Jones, A. R., & Feddema, J. J. (2010). Assessing spatiotemporal variability of drought in the US central plains. *Journal of Arid Environments*, *74*(2), 247–255. https://doi.org/10.1016/j.jaridenv.2009.08.008
Long, B., Zhang, B., & He, X. (2023). Asymmetric response of global drought and pluvial detection to the length of climate epoch. *Journal of Hydrology*, *625*, 130078. https://doi.org/10.1016/j.jhydrol.2023.130078
Lorenzo-Lacruz, J., Vicente-Serrano, S. M., González-Hidalgo, J. C., López-Moreno, J. I., & Cortesi, N. (2013). Hydrological drought response to meteorological drought in the Iberian Peninsula. *Climate Research*, *58*(2), 117–131. https://doi.org/10.3354/cr01177
Ma, F., Luo, L., Ye, A., & Duan, Q. (2019). Drought characteristics and propagation in the semiarid Heihe River Basin in northwestern China. *Journal of Hydrometeorology*, *20*(1), 59–77. https://doi.org/10.1175/jhm-d-18-0129.1
Markonis, Y., Kumar, R., Hanel, M., Rakovec, O., Máca, P., & AghaKouchak, A. (2021). The rise of compound warm-season droughts in Europe. *Science Advances*, *7*(6), eabb9668. https://doi.org/10.1126/sciadv.abb9668
McKee, T. B., Doesken, N. J., & Kleist, J. (1993). The relationship of drought frequency and duration to time scales. In *Proceedings of the 8th conference on applied climatology* (Vol. 17, pp. 179–183).
Nash, J. E., & Sutcliffe, J. V. (1970). River flow forecasting through conceptual models part I—A discussion of principles. *Journal of Hydrology*, *10*(3), 282–290. https://doi.org/10.1016/0022-1694(70)90255-6
Omer, A., Zhuguo, M., Zheng, Z., & Saleem, F. (2020). Natural and anthropogenic influences on the recent droughts in Yellow River Basin, China. *Science of the Total Environment*, *704*, 135428. https://doi.org/10.1016/j.scitotenv.2019.135428

Pan, M., & Wood, E. F. (2010). Impact of accuracy, spatial availability, and revisit time of satellite-derived surface soil moisture in a multiscale ensemble data assimilation system. *Ieee Journal of Selected Topics in Applied Earth Observations and Remote Sensing*, *3*(1), 49–56. https://doi.org/10.1109/jstars.2010.2040585

Peng, J., Dadson, S., Hirpa, F., Dyer, E., Lees, T., Miralles, D. G., et al. (2020). A pan-African high-resolution drought index dataset. *Earth System Science Data*, *12*(1), 753–769. https://doi.org/10.5194/essd-12-753-2020

Rangecroft, S., Van Loon, A. F., Maureira, H., Verbist, K., & Hannah, D. M. (2019). An observation-based method to quantify the human influence on hydrological drought: Upstream–downstream comparison. *Hydrological Sciences Journal*, *64*(3), 276–287. https://doi.org/10.1080/02626667.2019.1581365

Sattar, M. N., Lee, J. Y., Shin, J. Y., & Kim, T. W. (2019). Probabilistic characteristics of drought propagation from meteorological to hydrological drought in South Korea. *Water Resources Management*, *33*(7), 2439–2452. https://doi.org/10.1007/s11269-019-02278-9

Shah, D., Shah, H. L., Dave, H. M., & Mishra, V. (2021). Contrasting influence of human activities on agricultural and hydrological droughts in India. *Science of the Total Environment*, *774*, 144959. https://doi.org/10.1016/j.scitotenv.2021.144959

Shao, D., Chen, S., Tan, X., & Gu, W. (2018). Drought characteristics over China during 1980–2015. *International Journal of Climatology*, *38*(9), 3532–3545. https://doi.org/10.1002/joc.5515

Shiklomanov, I. A. (1997). Assessment of water resources and water availability in the world. In *Comprehensive assessment of the freshwater re-sources of the world*.

Shukla, S., & Wood, A. W. (2008). Use of a standardized runoff index for characterizing hydrologic drought. *Geophysical Research Letters*, *35*(2), L02405. https://doi.org/10.1029/2007gl032487

Steinfeld, H., Gerber, P., Wassenaar, T. D., Castel, V., Rosales, M., Rosales, M., & de Haan, C. (2006). *Livestock's long shadow: Environmental issues and options* (p. 37). Food & Agriculture Organization.

Sutanudjaja, E. H., Van Beek, R., Wanders, N., Wada, Y., Bosmans, J. H., Drost, N., et al. (2018). PCR-GLOBWB 2: A 5 arcmin global hydrological and water resources model. *Geoscientific Model Development*, *11*(6), 2429–2453. https://doi.org/10.5194/gmd-11-2429-2018

Tallaksen, L. M., Hisdal, H., & Van Lanen, H. A. (2009). Space–time modelling of catchment scale drought characteristics. *Journal of Hydrology*, *375*(3–4), 363–372. https://doi.org/10.1016/j.jhydrol.2009.06.032

Van Beek, L. P. H., Wada, Y., & Bierkens, M. F. (2011). Global monthly water stress: 1. Water balance and water availability. *Water Resources Research*, *47*(7). https://doi.org/10.1029/2010wr009791

Van Loon, A. F., Gleeson, T., Clark, J., Van Dijk, A. I., Stahl, K., Hannaford, J., et al. (2016). Drought in the anthropocene. *Nature Geoscience*, *9*(2), 89–91. https://doi.org/10.1038/ngeo2646

Van Loon, A. F., & Laaha, G. (2015). Hydrological drought severity explained by climate and catchment characteristics. *Journal of Hydrology*, *526*, 3–14. https://doi.org/10.1016/j.jhydrol.2014.10.059

Van Loon, A. F., Rangecroft, S., Coxon, G., Breña Naranjo, J. A., Van Ogtrop, F., & Van Lanen, H. A. (2019). Using paired catchments to quantify the human influence on hydrological droughts. *Hydrology and Earth System Sciences*, *23*(3), 1725–1739. https://doi.org/10.5194/hess-23-1725-2019

Van Loon, A. F., Van Huijgevoort, M. H. J., & Van Lanen, H. A. J. (2012). Evaluation of drought propagation in an ensemble mean of large-scale hydrological models. *Hydrology and Earth System Sciences*, *16*(11), 4057–4078. https://doi.org/10.5194/hess-16-4057-2012

Vörösmarty, C. J., Leveque, C., & Revenga, C. (2005). *Millennium ecosystem assessment volume 1: Conditions and trends, chap. 7: Freshwater ecosystems* (Vol. 135, pp. 165–207). Island Press.

Wada, Y., de Graaf, I. E., & van Beek, L. P. (2016). High-resolution modeling of human and climate impacts on global water resources. *Journal of Advances in Modeling Earth Systems*, *8*(2), 735–763. https://doi.org/10.1002/2015ms000618

Wada, Y., Van Beek, L. P., Wanders, N., & Bierkens, M. F. (2013). Human water consumption intensifies hydrological drought worldwide. *Environmental Research Letters*, *8*(3), 034036. https://doi.org/10.1088/1748-9326/8/3/034036

Wada, Y., Wisser, D., & Bierkens, M. F. (2014). Global modeling of withdrawal, allocation and consumptive use of surface water and groundwater resources. *Earth System Dynamics*, *5*(1), 15–40. https://doi.org/10.5194/esd-5-15-2014

Wan, W., Zhao, J., Li, H. Y., Mishra, A., Ruby Leung, L., Hejazi, M., et al. (2017). Hydrological drought in the anthropocene: Impacts of local water extraction and reservoir regulation in the US. *Journal of Geophysical Research: Atmospheres*, *122*(21), 11–313. https://doi.org/10.1002/2017jd026899

Wang, J., Sheng, Y., & Wada, Y. (2017). Little impact of the Three Gorges Dam on recent decadal lake decline across China's Yangtze plain. *Water Resources Research*, *53*(5), 3854–3877. https://doi.org/10.1002/2016wr019817

Wang, L. (1998). Changes of rainfall and runoff in the Yellow River (in Chinese). In *Influences of water discharge and sediments' changes on the Yellow River System, chap. 2* (pp. 13–14). Huanghe River Water Resour. Publ.

Wang, M., Jiang, S., Ren, L., Xu, C. Y., Yuan, F., Liu, Y., & Yang, X. (2020). An approach for identification and quantification of hydrological drought termination characteristics of natural and human-influenced series. *Journal of Hydrology*, *590*, 125384. https://doi.org/10.1016/j.jhydrol.2020.125384

Wei, L. Y., Jiang, S. H., Ren, L. L., Zhang, L., Wang, M., Liu, Y., & Duan, Z. (2022). Bias correction of GPM IMERG early run daily precipitation product using near real-time CPC global measurements. *Atmospheric Research*, *279*, 106403. https://doi.org/10.1016/j.atmosres.2022.106403

Wei, Z., He, X., Zhang, Y., Pan, M., Sheffield, J., Peng, L., et al. (2020). Identification of uncertainty sources in quasi-global discharge and inundation simulations using satellite-based precipitation products. *Journal of Hydrology*, *589*, 125180. https://doi.org/10.1016/j.jhydrol.2020.125180

Wilhite, D. A., Sivakumar, M. V., & Pulwarty, R. (2014). Managing drought risk in a changing climate: The role of national drought policy. *Weather and Climate Extremes*, *3*, 4–13. https://doi.org/10.1016/j.wace.2014.01.002

World Meteorological Organization. (2006). *Drought monitoring and warning: Concepts, progress and future challenges* (pp. 6–9). WMO Publication. No, 1006.

World Resources Institute (WRI). (1998). *World resources: A guide to the global environment 1998–1999*. World Resources Institute.

Wu, F., Yang, X., Cui, Z., Ren, L., Jiang, S., Liu, Y., & Yuan, S. (2024). The impact of human activities on blue-green water resources and quantification of water resource scarcity in the Yangtze River Basin. *Science of the Total Environment*, *909*, 168550. https://doi.org/10.1016/j.scitotenv.2023.168550

Wu, J., Chen, X., Yao, H., Gao, L., Chen, Y., & Liu, M. (2017). Non-linear relationship of hydrological drought responding to meteorological drought and impact of a large reservoir. *Journal of Hydrology*, *551*, 495–507. https://doi.org/10.1016/j.jhydrol.2017.06.029

Wu, J., Chen, X., Yao, H., & Zhang, D. (2021). Multi-timescale assessment of propagation thresholds from meteorological to hydrological drought. *Science of the Total Environment*, *765*, 144232. https://doi.org/10.1016/j.scitotenv.2020.144232

Wu, J., Liu, Z., Yao, H., Chen, X., Chen, X., Zheng, Y., & He, Y. (2018). Impacts of reservoir operations on multi-scale correlations between hydrological drought and meteorological drought. *Journal of Hydrology*, *563*, 726–736. https://doi.org/10.1016/j.jhydrol.2018.06.053

Wu, Z. Y., Lu, G. H., Wen, L., & Lin, C. A. (2011). Reconstructing and analyzing China's fifty-nine year (1951–2009) drought history using hydrological model simulation. *Hydrology and Earth System Sciences*, *15*(9), 2881–2894. https://doi.org/10.5194/hess-15-2881-2011

Xu, K., Yang, D., Xu, X., & Lei, H. (2015). Copula based drought frequency analysis considering the spatio-temporal variability in Southwest China. *Journal of Hydrology*, *527*, 630–640. https://doi.org/10.1016/j.jhydrol.2015.05.030

Xu, Y., Zhang, X., Hao, Z., Singh, V. P., & Hao, F. (2021). Characterization of agricultural drought propagation over China based on bivariate probabilistic quantification. *Journal of Hydrology*, *598*, 126194. https://doi.org/10.1016/j.jhydrol.2021.126194

Xu, Y., Zhang, X., Wang, X., Hao, Z., Singh, V. P., & Hao, F. (2019). Propagation from meteorological drought to hydrological drought under the impact of human activities: A case study in northern China. *Journal of Hydrology*, *579*, 124147. https://doi.org/10.1016/j.jhydrol.2019.124147

Yang, X., Zhang, M., He, X., Ren, L., Pan, M., Yu, X., et al. (2020). Contrasting influences of human activities on hydrological drought regimes over China based on high-resolution simulations. *Water Resources Research*, *56*(6), e2019WR025843. https://doi.org/10.1029/2019wr025843

Yu, C., Shao, H., Hu, D., Liu, G., & Dai, X. (2023). Merging precipitation scheme design for improving the accuracy of regional precipitation products by machine learning and geographical deviation correction. *Journal of Hydrology*, *620*, 129560. https://doi.org/10.1016/j.jhydrol.2023.129560

Yu, M., Li, Q., Hayes, M. J., Svoboda, M. D., & Heim, R. R. (2014). Are droughts becoming more frequent or severe in China based on the standardized precipitation evapotranspiration index: 1951–2010? *International Journal of Climatology*, *34*(3), 545–558. https://doi.org/10.1002/joc.3701

Yuan, X., Zhang, M., Wang, L., & Zhou, T. (2017). Understanding and seasonal forecasting of hydrological drought in the Anthropocene. *Hydrology and Earth System Sciences*, *21*(11), 5477–5492. https://doi.org/10.5194/hess-21-5477-2017

Zhang, D. D., Yan, D. H., Lu, F., Wang, Y. C., & Feng, J. (2015). Copula-based risk assessment of drought in Yunnan province, China. *Natural Hazards*, *75*(3), 2199–2220. https://doi.org/10.1007/s11069-014-1419-6

Zhang, T., Su, X., Zhang, G., Wu, H., Wang, G., & Chu, J. (2022). Evaluation of the impacts of human activities on propagation from meteorological drought to hydrological drought in the Weihe River Basin, China. *Science of the Total Environment*, *819*, 153030. https://doi.org/10.1016/j.scitotenv.2022.153030

Zhao, M., Huang, S., Huang, Q., Wang, H., Leng, G., & Xie, Y. (2019). Assessing socio-economic drought evolution characteristics and their possible meteorological driving force. *Geomatics, Natural Hazards and Risk*, *10*(1), 1084–1101. https://doi.org/10.1080/19475705.2018.1564706

Zhu, Y., Liu, Y., Wang, W., Singh, V. P., Ma, X., & Yu, Z. (2019). Three dimensional characterization of meteorological and hydrological droughts and their probabilistic links. *Journal of Hydrology*, *578*, 124016. https://doi.org/10.1016/j.jhydrol.2019.124016